

## MASTER

### Comparison of the orifice, inertance and double inlet pulse tube refrigerator

Aerts, S.C.M.

*Award date:*  
1999

[Link to publication](#)

#### **Disclaimer**

This document contains a student thesis (bachelor's or master's), as authored by a student at Eindhoven University of Technology. Student theses are made available in the TU/e repository upon obtaining the required degree. The grade received is not published on the document as presented in the repository. The required complexity or quality of research of student theses may vary by program, and the required minimum study period may vary in duration.

#### **General rights**

Copyright and moral rights for the publications made accessible in the public portal are retained by the authors and/or other copyright owners and it is a condition of accessing publications that users recognise and abide by the legal requirements associated with these rights.

- Users may download and print one copy of any publication from the public portal for the purpose of private study or research.
- You may not further distribute the material or use it for any profit-making activity or commercial gain

#### **Take down policy**

If you believe that this document breaches copyright please contact us providing details, and we will remove access to the work immediately and investigate your claim.

**Comparison of the orifice, inertance  
and double inlet pulse tube refrigerator**

by S.C.M. Aerts  
August 1999

Under supervision of  
ir. H.W.G. Hooijkaas  
ir. A.A.J. Benschop  
Prof. dr. A.T.A.M. de Waele

## Summary

In this report three types of miniature pulse tube coolers have been investigated: the orifice, the inertance and the double inlet pulse tube cooler. The focus has been on the characterization of the different types of pulse tubes and experimental verification of the pulse tube theory. Experiments with two pulse tube coolers have been done. In one cooler both the regenerator and pulse tube are 55 mm long and in the other both are 70 mm long. The warm end of both configurations can be modified. This makes it possible to do experiments with an orifice, an inertance and a double inlet pulse tube, with the same regenerator-tube combination. The influence of the orifice diameter, the inertance diameter and length, and the bypass orifice diameter has been investigated. Also the influence of the driving frequency, the mean pressure and the input power has been investigated.

It has been found that cooling power is mainly obtained by means of an adiabatic enthalpy flow through the core of the tube. The adiabatic enthalpy flow is linear with the cosine of the phase angle  $\theta_L$  at the low temperature side of the tube. The phase angle is the phase difference between the pressure and the volume flow. The optimal performance conditions are different for each type of pulse tube cooler. This also means that each type of pulse tube cooler has a different optimal phase angle. To increase the cooling power and/or to reach lower cold heat exchanger temperatures, the adiabatic enthalpy flow through the tube must be increased and/or the losses must be reduced. The adiabatic enthalpy flow can be increased by decreasing the optimal phase angle at the low temperature side of the tube. It has been found that in an orifice pulse tube the phase angle is between  $40^\circ$  and  $45^\circ$  when the best performing orifice is used. Lower temperatures have been reached with an inertance pulse tube. With an inertance pulse tube the phase angle has been found to be around  $30^\circ$  at the optimum inertance length. The use of a bypass orifice has been beneficial in both an orifice and an inertance pulse tube. With a bypass orifice lower cold heat exchanger temperatures have been reached. The losses can be reduced by decreasing the enthalpy flow through the regenerator and the heat conduction through the wall. The enthalpy flow through the regenerator decreases when the filling factor of the regenerator increases. It has been found that a filling factor of 0.22 is too low and that a filling factor of 0.29 gives better results. The heat conduction through the wall decreases as the temperature gradient in the wall decreases.

The lowest temperature reached in the experiments is 73 K. This has been reached with the 70 mm pulse tube which has a filling factor of 0.29. The inertance had a diameter of 1.02 mm and a length of 1.7 m, the bypass orifice had a diameter of 0.2 mm, the mean pressure was 2.8 MPa, the frequency 35 Hz and the mechanical input power 35 W.

## Preface

During the period October '98 to August '99, I carried out my graduation project at Signaal USFA. With this report, I present the final results.  
Everybody who helped to make my stay at Signaal USFA a very pleasant period:  
Thanks!

# Contents

## Summary

<b>List of symbols .....</b>	<b>3</b>
<b>Chapter 1 Introduction .....</b>	<b>5</b>
1.1 Basic pulse tube	5
1.2 Orifice pulse tube	6
1.3 Double inlet pulse tube	7
1.4 Inertance pulse tube	8
<b>Chapter 2 Theory.....</b>	<b>10</b>
2.1 Simplifications	10
2.2 Thermodynamics	10
2.3 Enthalpy flow through an adiabatic tube	13
2.4 Electrical analogue	16
2.4.1. Orifice pulse tube	16
2.4.2. Inertance pulse tube	18
2.4.3. Double inlet pulse tube	21
2.5 Enthalpy flow through an adiabatic tube with a thermal boundary layer	24
<b>Chapter 3 The experimental apparatus.....</b>	<b>28</b>
3.1 Refrigeration system	28
3.1.1. The regenerator	29
3.1.2. Orifices and inertances	31
3.2 Measuring system	31
3.3 Characterization of the orifices	32
<b>Chapter 4 The 55 mm pulse tube cooler .....</b>	<b>36</b>
4.1 The orifice pulse tube	36
4.2 The inertance pulse tube	45
4.3 The double inlet pulse tube	49
<b>Chapter 5 The 70 mm pulse tube cooler .....</b>	<b>51</b>
5.1 The orifice pulse tube	51
5.2 The inertance pulse tube	56
5.3 The double inlet pulse tube	58
<b>Chapter 6 Conclusions .....</b>	<b>61</b>
<b>References.....</b>	<b>65</b>

## List of symbols

$\langle \rangle$	time-average	[-]
$\alpha$	constant	[-]
$\delta$	boundary layer thickness	[m]
$\zeta$	friction coefficient	[-]
$\Delta$	difference	[-]
$\gamma$	ratio of isobaric to isochoric specific heats	[-]
$\theta$	phase angle between pressure oscillation and volume flow	[deg]
$\lambda$	heat conduction coefficient	[J·s <sup>-1</sup> m <sup>-1</sup> K <sup>-1</sup> ]
$\mu$	viscosity	[Pa·s]
$\xi$	coefficient of performance	[-]
$\rho$	density	[kg·m <sup>-3</sup> ]
$\tau$	period of the oscillation	[s]
$\phi$	volume flow	[m <sup>3</sup> s <sup>-1</sup> ]
$\omega$	angular frequency	[s <sup>-1</sup> ]
$a$	constant	[Pa·s]
$A$	cross-sectional area	[m <sup>2</sup> ]
$c_p$	isobaric heat capacity per unit mass	[J·kg <sup>-1</sup> K <sup>-1</sup> ]
$c_v$	isochoric heat capacity per unit mass	[J·kg <sup>-1</sup> K <sup>-1</sup> ]
$C$	volumetric capacity	[m <sup>3</sup> Pa <sup>-1</sup> ]
$C_0$	heat capacity per unit regenerator volume	[J·K <sup>-1</sup> m <sup>-3</sup> ]
$d$	diameter	[m]
$f$	frequency or filling factor	[s <sup>-1</sup> ] or [-]
$h$	specific enthalpy	[J·kg <sup>-1</sup> ]
$H$	enthalpy	[J]
$l$	length	[m]
$L$	inductance or regenerator/tube length	[Pa·s <sup>2</sup> m <sup>-3</sup> ] or [m]
$m$	mass	[kg]
$n$	number	[-]
$p$	pressure	[Pa]
$P$	power	[W]
$Q$	heat [J]	
$r$	radial co-ordinate	[m]
$R_m$	specific gas constant	[J·kg <sup>-1</sup> K <sup>-1</sup> ]
$R$	flow resistance or radius	[Pa·s·m <sup>-3</sup> ] or [m]
Re	real part of	[-]
$s$	specific entropy	[J·kg <sup>-1</sup> K <sup>-1</sup> ]
$S$	entropy	[J·K <sup>-1</sup> ]
$T$	temperature	[K]
$t$	time or distance	[s] or [m]
$U$	internal energy	[J]
$u$	axial velocity	[m·s <sup>-1</sup> ]
$V$	volume	[m <sup>3</sup> ]
$W$	work [J]	
$x$	axial co-ordinate	[m]

$X$	oscillating quantity	[-]
$Z$	flow impedance	[Pa·s·m <sup>-3</sup> ]

### Top-scripts, superscripts, subscripts

^	oscillating quantity
·	flow rate
*	complex conjugate
//	parallel
0	time-average
2	bypass orifice
55	55 mm pulse tube cooler
70	70 mm pulse tube cooler
ad	adiabatic
air	surroundings
b	buffer
b→t	buffer to tube
C	compressor
car	Carnot
crit	critical
d	gauze wire
flow	steady flow
g	gas
gr	gradient
H	high temperature
i	irreversible
im	imaginary
in	in
L	low temperature
mech	mechanical
min	minimum
opt	optimal
out	out
r	regenerator
re	real
su	surface
t	tube
t→b	tube to buffer
T	temperature
w	wall

# Chapter 1

## Introduction

Miniature cryocoolers are small refrigerators that reach temperatures below 120 K. These miniature refrigerators are mainly used to cool infrared detectors for remote sensing. New applications are appearing, like cooling semiconductors for high-speed digital circuits. Different types of cryocoolers exist like e.g. stirling and pulse tube refrigerators [1].

The pulse tube refrigerator is the subject of this report. An advantage of this cooler over the stirling cooler is that it contains no moving parts in the cold. As there are fewer moving parts, the amount of vibrations distributed to the cooled device is reduced. Makes it less sensitive for external influences, increasing the potential for a longer lifetime. Less moving parts makes it also mechanically simpler, reducing the construction costs. In recent years the efficiency of pulse tube coolers increased significant, so that nothing obstructs a commercial break through in the near future.

Since Gifford and Longworth [2] in 1963 invented a new type refrigerator, now called the basic pulse tube refrigerator (BPTR), a lot of research and improvements have been made. A significant improvement, which gave the research to pulse tubes a new impulse, was made by Mikulin et al. [3] in 1984. They introduced the orifice pulse tube refrigerator (OPTR). The efficiency improved with the introduction of the double inlet concept (DIPTR) in 1990 by Zhu et al. [4]. More stable results can be obtained with the inertance pulse tube (IPTR) introduced by Kanao et al. in 1994 [5]. Other types of pulse tube coolers exist, like two (or more) stage pulse tubes, pulse tubes with an expander and multibypass pulse tubes. These will not be discussed in this report.

### 1.1 Basic pulse tube

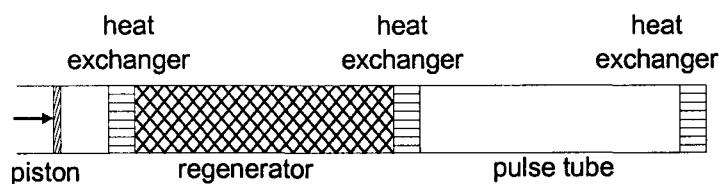


*figure 1.1: Schematics of the basic pulse tube refrigerator.*

The cooling principle of a basic pulse tube, as depicted in figure 1.1, is based on the transfer of heat between the working fluid and a surface. The actual pulse tube is empty and closed at the right. At the closed side a good heat transfer surface exists between the fluid and the surroundings in order to reject an amount of heat. The left side of the tube is open and is connected to a heat exchanger, which absorbs an amount of cooling power. With the aid of a compressor, a pressure oscillation is generated in the tube. The regenerator separates the compressor from the tube. The regenerator consists of a porous medium with a high heat capacity. It serves as a temperature barrier between the warm (left) side and the cold (right) side. It enforces locally isothermal conditions on



the fluid: during the compression phase (when the fluid moves to the pulse tube) heat is stored in the regenerator and this heat is rejected again during the expansion phase.

A fluid parcel moves towards the closed end of the tube during the pressure build-up phase. At the same time, it experiences a temperature rise due to adiabatic compression. In this situation, the temperature of the fluid is higher than the temperature of the surface, causing heat to flow from fluid to surface. If the pressure decreases again the fluid parcel moves back. The temperature of the fluid parcel drops due to adiabatic expansion. The temperature of the fluid is lower than the surface temperature, causing heat to flow from surface to fluid. The most left fluid parcel in the tube absorbs heat in the cold heat exchanger from the surroundings and transfers it a bit to the right. There another element picks it up and transfers it a bit further to the right until it finally reaches the heat exchanger at the closed end where the heat is rejected to the surroundings. This cooling principle is called surface heat pumping.

Surface heat pumping has a low temperature limit. If the temperature of the cold heat exchanger drops the temperature gradient of the tube's wall rises. The lower limit is reached when the temperature rise of a fluid parcel equals the temperature increase of the wall due to the displacement of the parcel. In this situation, there will be no heat flowing from fluid to surface, as their temperatures are the same. The temperature gradient at which this occurs is called the critical temperature gradient.

The velocity of the fluid leads the pressure oscillation by  $90^\circ$ . If the fluid moves right (the fluid velocity is defined as positive), the pressure increases. When the pressure is maximal the velocity is zero. The pressure decreases if the fluid moves left and has a negative velocity.

Note that this surface heat pumping mechanism requires that the compression and expansion processes are not completely adiabatic, but somewhere between isothermal and adiabatic. It also requires that the fluid leaving the regenerator has the same temperature as the low temperature heat exchanger. If the fluid leaving the regenerator has a higher temperature than the cold heat exchanger, heat is rejected. The cooling power is lowered with the amount of heat that is rejected.

## 1.2 Orifice pulse tube

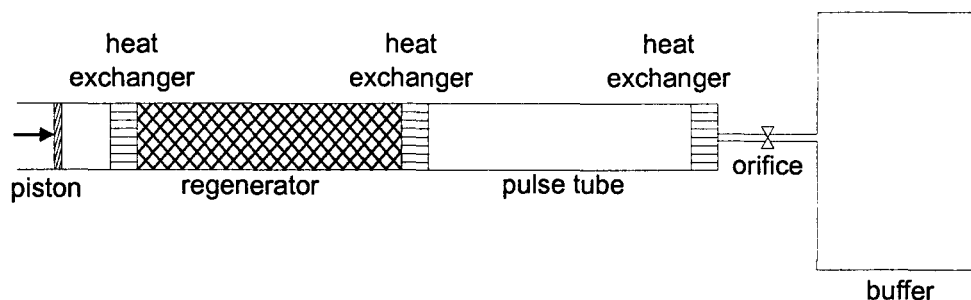


*figure 1.2: Schematics of the orifice pulse tube refrigerator.*

The orifice pulse tube as shown in figure 1.2, has an orifice and a buffer volume behind the formerly closed end. The orifice is a flow resistance that allows some of the fluid in the tube to enter the large buffer volume placed behind the orifice. The cooling mechanism is quite different from basic pulse tube cooling. In the orifice pulse tube cooler there is an adiabatic enthalpy flow through the tube, to the orifice-buffer configuration. In the orifice, the adiabatic enthalpy flow is dissipated. The adiabatic enthalpy flow generates much more cooling power than surface heat pumping.

Analogous to the basic pulse tube, a fluid parcel moves to the right during the pressure build-up phase. However, the phase difference between the velocity of the fluid and the pressure oscillation will not be  $90^\circ$ , as at the warm side of the tube fluid is leaving through the orifice. The velocity of the fluid flowing through the orifice is in-phase with the pressure oscillation in the tube. The velocity of the fluid entering the tube for the pressure build-up leads the pressure oscillation by  $90^\circ$ . Combination of these two gives the orifice pulse tube a phase difference with some intermediate angle. Part of the fluid at the low temperature side of the tube has a velocity in-phase with the pressure oscillation. In-phase means that the fluid is first compressed, moves to the right, where it expands after which it moves back to the left. As the parcel is compressed, energy is put in the parcel and as no energy can flow through the regenerator, this must be absorbed from the surroundings in the cold heat exchanger. This energy is dissipated in the orifice. In this situation not only the fluid near the surface contributes to the cooling effect but all the fluid in the tube.

### 1.3 Double inlet pulse tube

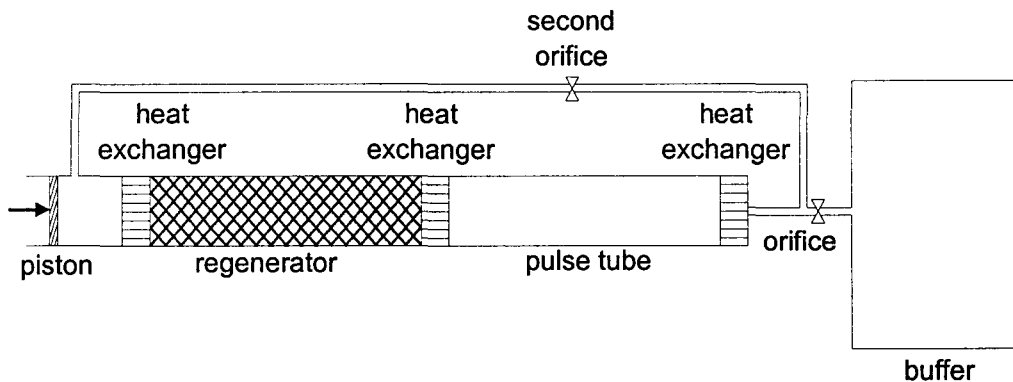


*figure 1.3: Schematics of the double inlet pulse tube refrigerator.*

Until now, we assumed that the temperature of the fluid leaving the regenerator is the same as the temperature of the cold heat exchanger. This is true for an ideal regenerator. In reality, there will be a temperature difference between the fluid and the local regenerator temperature, causing an enthalpy flow through the regenerator. To lower this loss in cooling power the enthalpy flow through the regenerator should be as low as possible.

In the former section was stated that an orifice pulse tube creates cooling power by means of an adiabatic enthalpy flow but that there is still surface heat pumping. In general, the temperature gradient of the wall is larger than the critical temperature gradient. The compressed fluid parcel absorbs heat from the surface and transfers it from the warm to the cold end.

A bypass orifice is added to decrease the enthalpy flow through the regenerator and at the same time decrease the displacement of a fluid parcel in the tube. With the bypass orifice the flow needed to compress and expand the fluid in the pulse tube is taken directly from the compressor instead of first passing the regenerator. In this situation the fluid in the tube is compressed and expanded in two directions, so fluid elements that enter the pulse tube at the cold end are compressed within a shorter range of displacement.

Another advantage of the bypass orifice is the larger pressure amplitude in the tube. The regenerator has a flow resistance, causing a pressure difference over the regenerator. If a

bypass orifice is added, an extra flow resistance is added parallel to the resistance of the regenerator. The sum of these two leads to a smaller impedance of the total system. The pressure drop between compressor and tube decreases, resulting in a larger pressure oscillation in the tube.

## 1.4 Inertance pulse tube

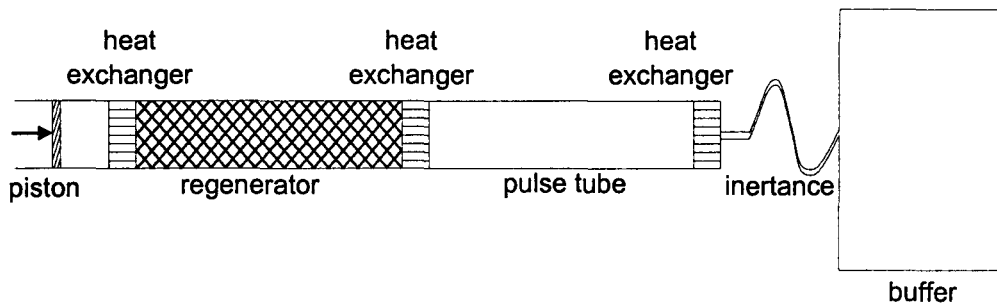


*figure 1.4: Schematics of the inertance pulse tube refrigerator.*

Another way to decrease the enthalpy flow through the regenerator and the displacement of the fluid in the tube is with the aid of an inertance. The inertance is a long capillary placed between the pulse tube and the buffer volume. The word “inertance” is an acoustics term formed by the combination of the words inertia and inductance. The inertia of the moving fluid has a positive effect on the cooling power and it is the acoustic analogue of an electrical inductance.

In the orifice pulse tube, the adiabatic enthalpy flow through the tube is simply dissipated in the orifice. In the inertance, the energy is not only dissipated, but the fluid in the inertance behaves as a gas spring. Due to the inertia of the fluid in the inertance, the fluid is still moving to the left as the fluid in the tube is already being compressed. When the fluid in the tube is expanded, the fluid in the inertance is still moving right. In this situation, a fluid element in the tube moves less during both the compression and the expansion phase than in the same situation in an orifice pulse tube.

The inertance can also be combined with a bypass orifice. The displacement of a fluid parcel in the tube will decrease a bit more, and the pressure amplitude in the tube increases.

Several years ago, Signaal USFA started a research program to develop a miniature pulse tube refrigerator, next to the miniature stirling coolers they already produce. During my graduation the main focuses has been on the characterization of different types of pulse tubes and experimentally verify the pulse tube theory.

Chapter 2 starts with a simple model for the pulse tube. For an adiabatic tube, the enthalpy flow through the tube has been deduced and discussed for the different pulse tube configurations. After that, the enthalpy flow has been deduced for a tube with an adiabatic core and a thermal boundary layer. Experiments have been done with two pulse tube coolers. The coolers are for the greatest part the same, but have some important differences. The warm end of both tubes can be modified. This makes it possible to do experiments with an orifice, an inertance and a double inlet pulse tube, with the same regenerator-tube combination. A description of both coolers has been given in chapter 3. In this chapter, the measuring devices have also been described and the orifices are characterized. A number of experiments have been done to see the

influence of the orifice diameter, the inertance diameter and length and the bypass orifice diameter. The driving frequency, the mean pressure and the input power have also been varied. In chapter 4, the experiments with the 55 mm pulse tube cooler have been discussed. This cooler has a regenerator and pulse tube with both a length of 55 mm. The regenerator has a filling factor of 0.22. The experiments with the 70 mm pulse tube cooler have been discussed in chapter 5. In this cooler, the regenerator has a filling factor of 0.29. The conclusions and recommendations have been given in chapter 6.

# Chapter 2

## Theory

In this chapter, a simple model for the pulse tube will be deduced. First, the pulse tube is considered adiabatic. For this situation the adiabatic enthalpy flow will be deduced and discussed for the different pulse tube configurations. In the last section, the thermal interaction with the wall will be taken into account. This introduces surface heat pumping and the gradient effect.

### 2.1 Simplifications

First, some simplifications are made. Although not completely correct, the derived model describes the general behaviour of the pulse tube cooler well.

- The working fluid is regarded as an ideal gas. As the used gas is helium, this will not give any problems for temperatures above 60 K.
- The pressure is uniform over the entire tube. The wavelength is around twenty metres for frequencies between 30 and 50 Hz, which is much longer than the length of the tube.
- The pressure drop due to viscosity in the tube is negligible.
- The velocity is regarded to be uniform over each cross-section in the tube and is much smaller than the speed of sound. This latter assumption allows linearization.
- Axial thermal conduction in the gas is neglected.
- The kinetic and potential energy in the tube is negligible.
- Gravitational acceleration is negligible small.

### 2.2 Thermodynamics

The first law of thermodynamics deals with energy conservation of a control volume. For an open system, as depicted in figure 2.1, the change in internal energy  $U$  of a control volume with fixed boundaries can be written as [6]:

$$\frac{dU}{dt} = \dot{Q} + \dot{W} + \dot{H}_{in} - \dot{H}_{out}. \quad (2.1)$$

The internal energy  $U$  is related to the heat flow  $\dot{Q}$  into the volume, the work  $\dot{W}$  done by external forces on the volume and the enthalpy flows  $\dot{H}$  across the boundaries of the volume.

The fluid oscillates and consequently all thermodynamic quantities vary in time. The time-average (denoted with  $\langle \rangle$ ) of an oscillating quantity  $X$  is

$$\langle X \rangle = \frac{1}{\tau} \int_t^{t+\tau} X dt', \quad (2.2)$$

with  $\tau$  the period of the oscillation.

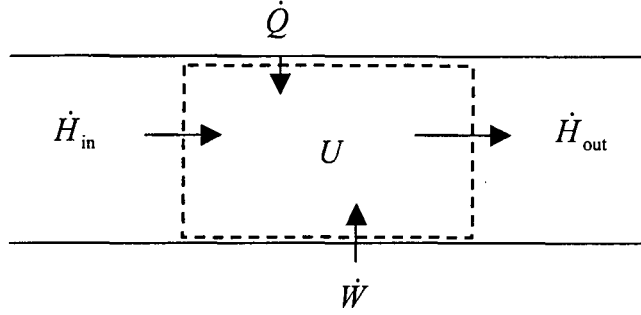


figure 2.1: Schematics of the first law of thermodynamics for an open system.

In steady state, the properties of the system are after one complete cycle the same as at the beginning of the cycle. This means that the average internal energy in the volume must be constant. Taking the time-average of equation (2.1) the term on the left side is zero and

$$\Delta\langle\dot{H}\rangle = \langle\dot{H}_{\text{out}}\rangle - \langle\dot{H}_{\text{in}}\rangle = \langle\dot{Q}\rangle + \langle\dot{W}\rangle. \quad (2.3)$$

The enthalpy flow can be written as the product of the mass flow  $\dot{m}$  across the boundary of the volume and the specific enthalpy  $h$ . For an ideal gas the specific enthalpy is the product of the isobaric specific heat  $c_p$  and the temperature  $T$

$$\dot{H} = \dot{m}h = \dot{m}c_p T. \quad (2.4)$$

The time-averaged enthalpy flow for an oscillating flow with period  $\tau=2\pi/\omega$  and  $\omega$  the angular frequency is

$$\begin{aligned} \langle\dot{H}\rangle &= c_p \langle\dot{m}T\rangle \\ &= \frac{c_p}{2\pi/\omega} \int_t^{t+2\pi/\omega} \dot{m}T dt. \end{aligned} \quad (2.5)$$

As in steady state there cannot be a net mass flow,  $\langle\dot{m}\rangle = 0$ , there will be an enthalpy flow due to temperature differences. The gas passing the boundary in one direction has a different temperature than the gas passing the boundary in the opposite direction.

The second law of thermodynamics deals with the change of entropy of a control volume. The time-average is defined analogous to equation (2.3) [6]

$$\Delta\langle\dot{S}\rangle = \frac{\langle\dot{Q}\rangle}{T} + \langle\dot{S}_i\rangle. \quad (2.6)$$

In this equation is  $\Delta\langle\dot{S}\rangle$  the difference between the entropy flow leaving and entering the control volume across the boundaries,  $\langle\dot{S}_i\rangle$  the entropy production rate due to irreversibility's and  $T$  the temperature of the gas at the position the heat flow is entering the volume.

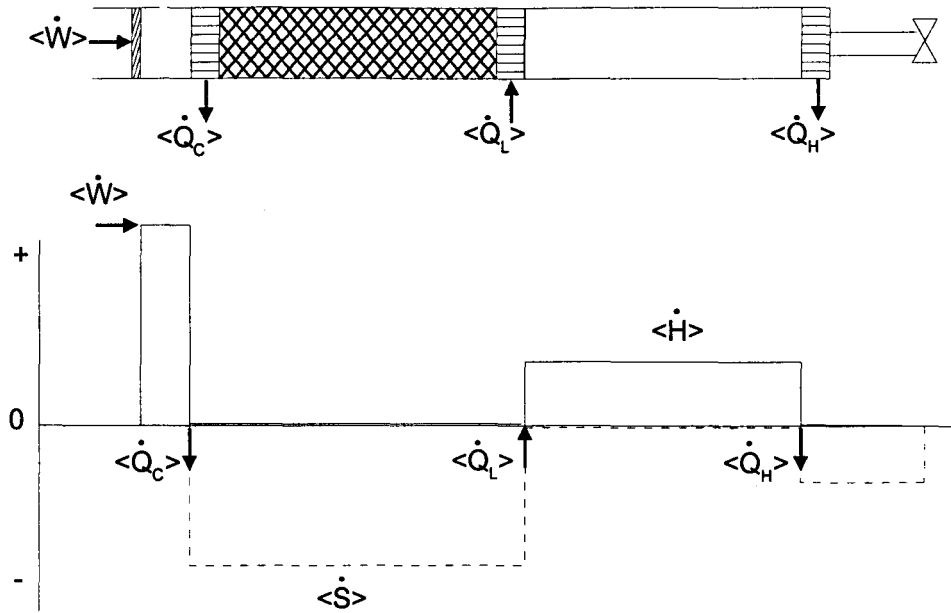


figure 2.2: Ideal pulse tube refrigerator with isothermal heat exchangers, locally isothermal regenerator and with an adiabatic tube, orifice/inertance, buffer and compressor. In the graph, the enthalpy and entropy flows are depicted schematically.

The ideal pulse tube cooler, as depicted in figure 2.2, is divided in subsystems that are adiabatic or isothermal. For each subsystem, the first or second law is applied. It is assumed that the heat flows are only non-zero in the heat exchangers and entropy is only produced in the orifice/inertance [7].

Both the enthalpy and entropy flow is zero in the buffer volume. In the adiabatic buffer, both the temperature and pressure are constant and no external work is done. An amount of entropy  $\langle \dot{S}_{in} \rangle$  is produced in the orifice/inertance as energy is dissipated at a temperature  $T_H$ . There must be an entropy flow,  $\langle \dot{S}_H \rangle = \langle \dot{S}_{in} \rangle$ , to the warm heat exchanger as the entropy flow to the buffer is zero. At the warm heat exchanger, heat is rejected to the surroundings:  $\langle \dot{Q}_H \rangle = T_H \langle \dot{S}_H \rangle$  because all processes in the tube occur adiabatically and reversibly. According to the first law, there must be an enthalpy flow  $\langle \dot{H} \rangle = \langle \dot{Q}_H \rangle$  in the tube. The enthalpy flow is constant through every cross-section of the tube. The enthalpy flows to the warm heat exchanger as the gas flows to the right with high pressure thus high temperature and to the left with low pressure thus low temperature. At the cold heat exchanger, an amount of heat  $\langle \dot{Q}_L \rangle = \langle \dot{H} \rangle$  is absorbed, as there cannot be an enthalpy flow through the regenerator. The regenerator is locally isothermal, when the gas flows to the right it has the same temperature as when it passes the cross-section flowing left. According to the second law there must be an entropy flow,  $\langle \dot{S}_L \rangle = \langle \dot{Q}_L \rangle / T_L$ . The entropy flows from the cold to the warm side of the regenerator. Heat is rejected at the warm heat exchanger due to the adiabatic compressor:  $\langle \dot{Q}_c \rangle = T_H \langle \dot{S}_L \rangle$ . There is an enthalpy flow  $\langle \dot{H} \rangle = \langle \dot{Q}_c \rangle$  from the piston to the heat exchanger. This is equal to the work  $\langle \dot{W} \rangle = \langle \dot{H} \rangle$  the compressor has to deliver to the system.

In figure 2.2 the enthalpy and entropy flows are depicted schematically, with a flow going to the right defined as positive. The enthalpy flow is positive as it flows from left to right and the entropy flow is negative as it flows in the opposite direction.

The coefficient of performance  $\xi$  of a refrigerator is defined as the ratio of the obtained time-average cooling power to the time-average work input in the system [6]

$$\xi = \frac{\langle \dot{Q}_L \rangle}{\langle \dot{W} \rangle} = \frac{T_L}{T_H}. \quad (2.7)$$

This equation shows that the efficiency of an ideal pulse tube cooler is lower than the efficiency of a Carnot cycle  $\xi_{\text{car}}=T_L/(T_H-T_L)$ . This is the direct result of the energy dissipation in the orifice. The energy dissipation is irreversible. Irreversible cycles can never reach the Carnot efficiency, but if  $T_L$  decreases, the pulse tube performance converges to the Carnot performance.

### 2.3 Enthalpy flow through an adiabatic tube

In this section, the enthalpy flow through a certain cross-section  $A_t$  of the tube is calculated. The mass flow is the product of the density  $\rho$ , the velocity of the fluid  $u$  and the cross-sectional area  $A_t$ . This combined with the equation of state for an ideal gas  $p/\rho=R_m T$  gives for the enthalpy flow (equation (2.5))

$$\langle \dot{H} \rangle = \frac{c_p A_t}{R_m} \langle pu \rangle. \quad (2.8)$$

In steady state, and in the pulse tube, the thermodynamic variables can be written as the sum of a mean and a harmonically in time varying part. Complex notation for the time-oscillatory quantities will be used in this report. However, only the real part of a complex solution represents the actual, physical solution.

For example the pressure  $p$ , density  $\rho$ , and temperature  $T$  are written as:

$$\begin{aligned} p &= p_0 + \hat{p}e^{i\alpha t}, \\ \rho &= \rho_0 + \hat{\rho}e^{i\alpha t}, \\ T &= T_0 + \hat{T}e^{i\alpha t}. \end{aligned} \quad (2.9)$$

The mean value (denoted with a subscript 0) is real. In general, the quantity of the time varying part (denoted with a  $\hat{\phantom{x}}$  on top) is complex due to the phase differences between the oscillating quantities.

In steady state, the time-averaged mass flow is equal to zero:  $\langle \dot{m} \rangle = A \langle \rho u \rangle = 0$ , or with equation (2.9)

$$\rho_0 u_0 + \langle \hat{\rho} \hat{u} \rangle = 0. \quad (2.10)$$

The tube is considered as adiabatic, for which Poisson's equation applies [6]:  $p/\rho^\gamma = \text{constant}$  and



$$\frac{d\rho}{\rho} = \frac{dp}{\gamma p}, \quad (2.11)$$

with  $\gamma$  the ratio of isobaric to isochoric specific heat,  $\gamma=c_p/c_v$ .

With the condition that the fluctuations are small in comparison to the mean values the mean velocity can be written as

$$u_0 = -\frac{\langle \hat{\rho} \hat{u} \rangle}{\rho_0} = -\frac{\langle \hat{p} \hat{u} \rangle}{\gamma p_0}. \quad (2.12)$$

As  $\rho_0 \gg \hat{\rho}$ , the equation implies that the mean velocity is much smaller than the oscillating velocity.

Substitution of equation (2.12) in equation (2.8) gives the enthalpy flow through an adiabatic tube

$$\begin{aligned} \langle \dot{H} \rangle &= \frac{c_p}{R_m} A_t [p_0 u_0 + \langle \hat{p} \hat{u} \rangle] \\ &= \frac{c_p}{R_m} A_t \left[ -\frac{\langle \hat{p} \hat{u} \rangle}{\gamma} + \langle \hat{p} \hat{u} \rangle \right]. \end{aligned} \quad (2.13)$$

The specific gas constant is equal to the difference between the isobaric to isochoric specific heat,  $R_m=c_p-c_v$ . Substitution results in the following equation for the time-averaged enthalpy flow is:

$$\langle \dot{H} \rangle = A_t \langle \hat{p} \hat{u} \rangle. \quad (2.14)$$

The time-averaged product of two complex quantities is half of the real part of the product. Where the product is taken between one complex quantity and the complex conjugation of the other quantity (denoted with a  $*$ )

$$\langle \dot{H} \rangle = \frac{1}{2} A_t \cdot \text{Re}[\hat{p} \hat{u}^*]. \quad (2.15)$$

If the enthalpy flow through the tube is analysed, this will usually be done with the phase angle  $\theta$ , which is the phase difference between pressure and velocity. With the phase angle  $\theta$ , the enthalpy flow can be written in the following final form:

$$\begin{aligned} \langle \dot{H} \rangle &= \frac{1}{2} A_t |\hat{p}| |\hat{u}| \cos \theta \\ &= \frac{1}{2} |\hat{p}| |\hat{\phi}| \cos \theta, \end{aligned} \quad (2.16)$$

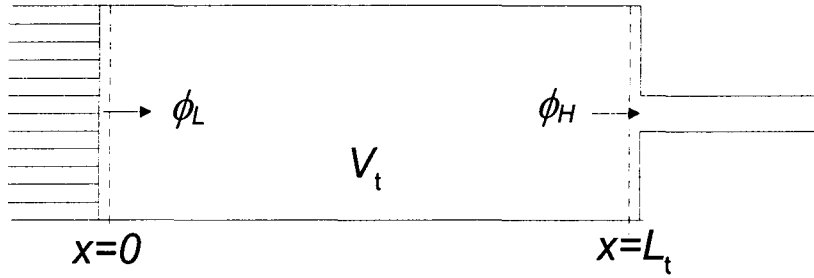


figure 2.3: Schematic overview of the volume flows in the pulse tube.

with  $|\hat{\phi}|$  the amplitude of the volume flow at the considered cross-section. Equation (2.16) shows that only the part of the volume flow in-phase with the pressure oscillation causes an enthalpy flow and thus cooling power.

Now the volume flows in the pulse tube will be considered further. For this the continuity equation [8] is written in the following form:

$$\frac{1}{\rho} \frac{d\rho}{dt} = -\frac{\partial u}{\partial x}. \quad (2.17)$$

Substitution of equation (2.11) in the continuity equation gives

$$\frac{\partial u}{\partial x} = -\frac{1}{\gamma p} \frac{\partial p}{\partial t}. \quad (2.18)$$

Multiplying both sides with  $A_t$  gives on the left side the derivative of the volume flow. The volume flow at a position  $x$  can be determined if equation (2.18) is integrated. In linearized form this results in

$$\begin{aligned} \phi(x,t) &= \phi_H(L_t,t) + \frac{A_t}{\gamma p} \frac{\partial p}{\partial t} (L_t - x) \\ &= \phi_H(L_t,t) + i\omega \frac{A_t \hat{p} e^{i\omega t}}{\gamma p_0} (L_t - x). \end{aligned} \quad (2.19)$$

$\phi_H(L_t,t)$  is the volume flow leaving the tube at the high temperature side, see figure 2.3. The amplitude of the volume flow  $\phi_L(0,t) = \hat{\phi}_L e^{i\omega t}$  entering the tube at the low temperature side is

$$\hat{\phi}_L = \hat{\phi}_H + i\omega \frac{V_t \hat{p}}{\gamma p_0}, \quad (2.20)$$

with  $V_t$  the volume of the tube. Substitution of this oscillating volume flow in equation (2.16) gives the time-averaged enthalpy flow at the low temperature side of the adiabatic tube

$$\begin{aligned} \langle \dot{H} \rangle &= \frac{1}{2} |\hat{p}| |\hat{\phi}_L| \cos \theta_L \\ &= \frac{1}{2} |\hat{p}| |\hat{\phi}_L|. \end{aligned} \quad (2.21)$$

Only that part of the volume flow in-phase with the pressure  $|\hat{\phi}_H|$ , contributes to the adiabatic enthalpy flow. According to the first law, the enthalpy flow is independent of the  $x$  position in the adiabatic tube. The pressure amplitude is constant throughout the tube, thus the parallel component of the volume flow must also be constant.

## 2.4 Electrical analogue

In this section, the pulse tube cooler is modelled like an electrical circuit. This is allowed as the system is much smaller than the wavelength of the pressure oscillation. The cooler is considered as a system of lumped elements. Each element has a flow impedance  $Z$ . The pressure is equivalent to an electric voltage and the volume flow to an electric current

$$\Delta\hat{p} = Z\hat{\phi}. \quad (2.22)$$

The tube's volume is described with a capacity  $C_t$ , because the tube has a finite volume in which gas accumulates, see equation (2.20):  $C_t = V_t/\gamma p_0$ . The buffer volume is also described with a capacity  $C_b$ .

### 2.4.1. Orifice pulse tube

In figure 2.4, the electrical analogue of the orifice pulse tube is depicted. Only the part after the cold heat exchanger is taken into account. The compressor generates a pressure  $p_t^1$  and volume flow  $\phi_L$  at the low temperature side of the tube. The orifice is represented by an impedance with resistance  $R$ . Through the orifice a volume flow  $\phi_b$  enters the buffer volume. The orifice has a very small volume, so the flow entering the buffer volume is equal to the flow leaving the tube at the high temperature side,  $\phi_H$  of equation (2.20).

The analysis is started in the buffer, as the buffer has only one opening through which gas can enter or leave it. Applying equation (2.22) on the buffer capacity, with an impedance  $Z=1/i\omega C_b$ , and the resistance, with  $Z=R$ , gives:

$$\begin{aligned} \hat{p}_b &= \frac{1}{i\omega C_b} \hat{\phi}_H, \\ \hat{p}_t - \hat{p}_b &= R\hat{\phi}_H. \end{aligned} \quad (2.23)$$

Substitution of the first equation in the second gives:

$$\hat{p}_t = \left(R + \frac{1}{i\omega C_b}\right)\hat{\phi}_H \cong R\hat{\phi}_H. \quad (2.24)$$

Due to the relative large volume of the buffer, the buffer capacity can be neglected in this equation. The volume flow leaving the tube and the pressure amplitude in the tube are in-phase, so  $\hat{\phi}_H = \hat{\phi}_H$ . The pressure in the buffer lags the pressure in the tube by  $90^\circ$ ,

---

<sup>1</sup> The pressure amplitude in the pulse tube is chosen to be real, so  $|\hat{p}_t| = \hat{p}_t$ .

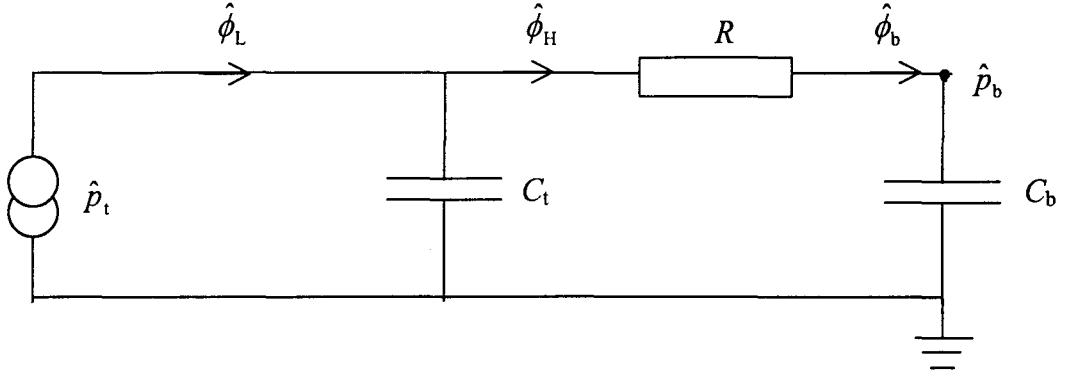


figure 2.4: Schematic overview of the orifice pulse tube after the cold heat exchanger. The orifice is depicted as a resistance  $R$ , the tube as a capacity  $C_t$  and the buffer as a capacity  $C_b$ .

as the volume flow leaving the tube at the warm end causes the pressure build-up in the buffer. As the buffer is large this also means that the pressure amplitude in the buffer volume will be small compared to the pressure amplitude in the tube.

The regenerator has also a resistance, which is neglected in the analyses. The volume flow at the cold side of the tube is taken constant; in which case the dissipation in the regenerator is constant. When the double inlet pulse tube is analysed the regenerator cannot be neglected as gas can enter the tube without first passing the regenerator.

The enthalpy flow can be expressed in terms of the present electrical components and the volume flow at the cold side

$$\begin{aligned} \langle \dot{H} \rangle &= \frac{1}{2} \text{Re}[\hat{p}_t \hat{\phi}_L^*] \\ &= \frac{1}{2} \text{Re}\left[\frac{R}{1+i\omega RC_t}\right] |\hat{\phi}_L|^2. \end{aligned} \quad (2.25)$$

With the right combination of  $\omega$ ,  $R$  and  $C_t$ , the enthalpy flow will be maximal. It can be shown by differentiation of equation (2.25) to  $R$ , for a fixed volume flow, that this is the case when

$$R_{\text{opt}} = \frac{1}{\omega C_t}. \quad (2.26)$$

This means that the phase angle  $\theta_L$  between the pressure and the volume flow at the cold side of the tube is  $45^\circ$ . This can be understood with equation (2.21). If the flow resistance increases the amount of gas flowing through the orifice decreases and the pressure amplitude in the tube increases. However, in the limit of an infinite large flow resistance this means that  $\hat{\phi}_H$  becomes zero and thus the enthalpy flow also. The phase angle  $\theta_L$  is  $90^\circ$ . If the flow resistance decreases the amount of gas flowing through the orifice increases and the pressure amplitude in the tube decreases. In the limit of no flow resistance the pressure amplitude  $\hat{p}_t$  becomes zero. The phase angle  $\theta_L$  is now  $0^\circ$ . The optimal situation will be somewhere in the middle. According to equation (2.26) even exactly in the middle.

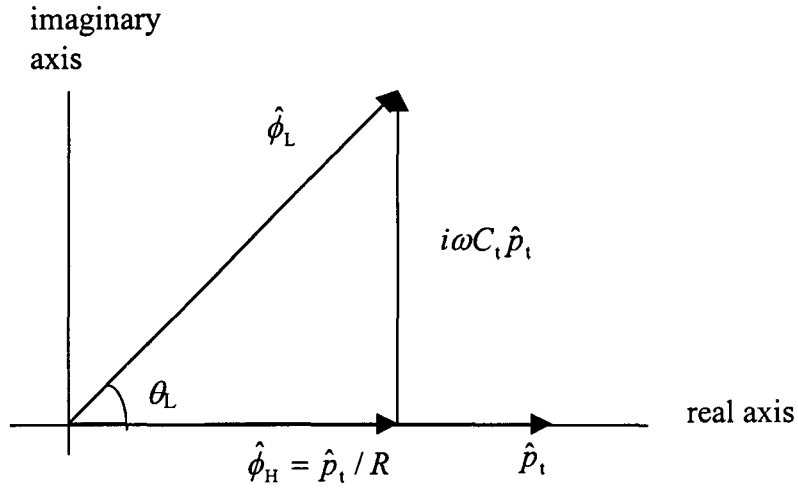


figure 2.5: Phasor diagram, illustrating the volume flows in the tube of an orifice pulse tube cooler.

In figure 2.5 this situation is depicted in a phasor diagram. In the optimal situation only half of the gas entering the tube at the low temperature side contributes to the enthalpy flow.

The optimal enthalpy flow is with figure 2.5 and equations (2.25) and (2.26)

$$\langle \dot{H} \rangle_{\text{opt}} = \frac{\hat{p}_t^2}{2R_{\text{opt}}}. \quad (2.27)$$

The enthalpy flow and thus the gross cooling power of a pulse tube refrigerator could increase if in the optimal situation the phase angle  $\theta_L$  would be smaller. The same volume flow  $\phi_L$  and pressure  $p_t$  will result in a larger enthalpy flow.

#### 2.4.2. Inertance pulse tube

In the inertance pulse tube, the phase shift due to the pressure build-up in the tube is partly counter balanced by the introduction of an inductance  $L$ . In practice, there is probably no equivalent to a pure self-inductance. We use capillaries, which are the combination of a resistance and an inductance, see figure 2.6.

The volume flow  $\phi_b$ , entering the buffer volume is both in amplitude and phase not the same as the volume flow  $\phi_H$ , entering the inertance from the tube side. Some of the gas accumulates in the inertance, introducing a phase shift. The accumulation of gas in the inertance will be neglected in the following analysis, so  $\hat{\phi}_H = \hat{\phi}_b$ .

The order of the resistance and inductance in figure 2.6 is arbitrary. In fact, the inertance is a series of infinite resistance/inductance combinations. Equation (2.22) is applied on the inertance, in which the impedance of an inductance is  $Z=i\omega L$

$$\hat{p}_t - \hat{p}_b = (R + i\omega L)\hat{\phi}_b. \quad (2.28)$$

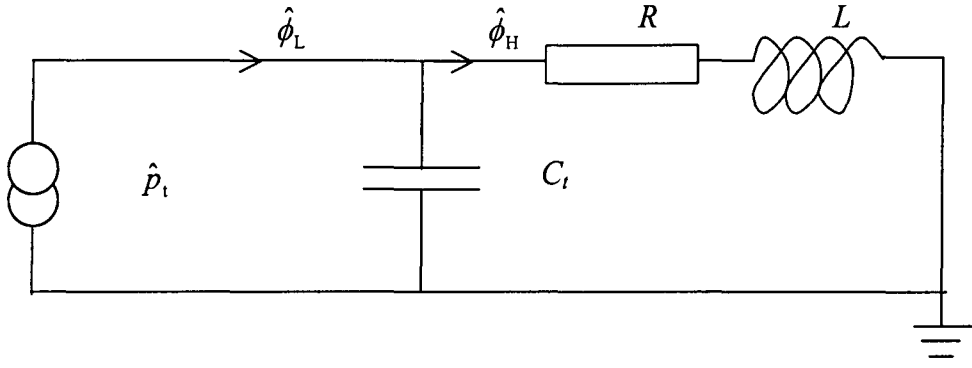


figure 2.6: Schematic overview of part of the pulse tube refrigerator after the cold heat exchanger with the inertance depicted as the resistance  $R$  and inductance  $L$ .

The equation shows that the phase difference between the pressure in the tube and buffer is larger than in the orifice pulse tube (equation (2.23)). As the phase difference is larger than  $90^\circ$ , the pressure in the buffer is still increasing (gas flows into the buffer) as the gas in the tube is expanded (gas flows from the tube to the regenerator). The gas in the tube is expanded in two directions until the pressure in the buffer starts decreasing. During part of the compression phase in the tube, the pressure in the buffer is still decreasing, as there is gas flowing from the buffer to the tube.

Both the resistance and the inductance of the inertance are dependent of its length  $l$  and diameter  $d$ . For laminar flows the resistance is [9]

$$R = \frac{128\mu l}{\pi d^4}, \quad (2.29)$$

with  $\mu$  the viscosity of the gas. The inertia of moving gas in a tube gives an inductance

$$L = \frac{4\rho l}{\pi d^2}. \quad (2.30)$$

These two relations give an indication about the behaviour of the flow in the inertance. The flow resistance will increase more than the inductance if the diameter of the inertance decreases. Notice that the inductance is dependent on the gas density and the flow resistance not. Several mean pressures will give just as many resistance/inductance combinations. Increasing the mean pressure increases the inductance while the flow resistance is unaffected.

The enthalpy flow is expressed in terms of the present electrical components and the volume flow at the cold side

$$\langle \dot{H} \rangle = \frac{1}{2} \operatorname{Re} \left[ \frac{R + i\omega L}{i\omega C_t (R + i\omega L) + 1} \right] |\hat{\phi}_L|^2. \quad (2.31)$$

Since  $L$  and  $R$  are fixed by the physical dimensions and gas characteristics, they cannot be chosen completely independent. To make things not to complicated we will assume that the resistance can be chosen independent of the inductance.

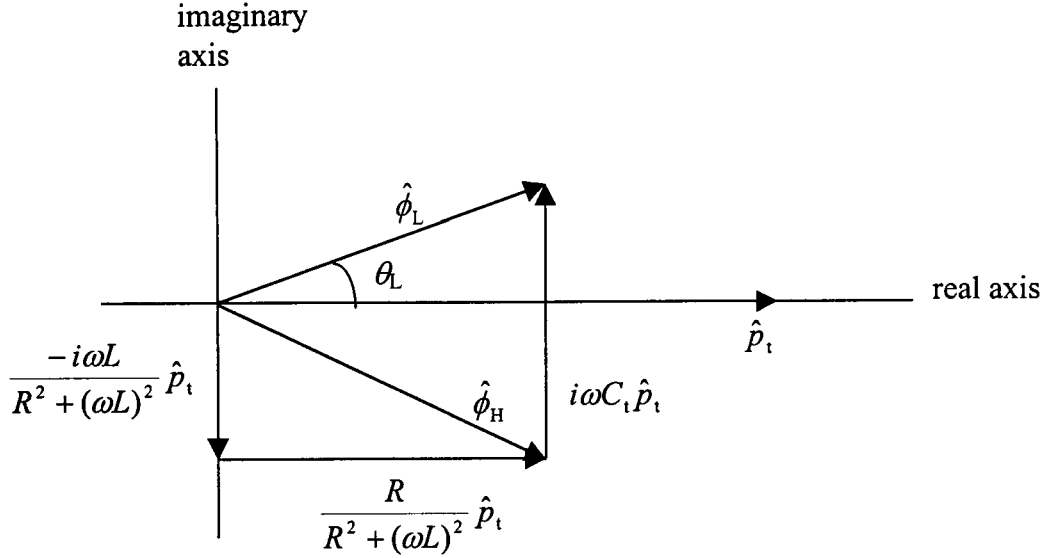


figure 2.7: Phasor diagram, illustrating the volume flows in the tube and inductance of an inductance pulse tube cooler.

With the right combination of  $\omega$ ,  $R$ ,  $L$  and  $C_t$ , the enthalpy flow will be maximal. Differentiation of equation (2.31) to  $R$ , for a fixed volume flow, gives the following relation

$$R_{\text{opt}} = \frac{1}{\omega C_t} - \omega L. \quad (2.32)$$

This equation shows immediately that for an inductance pulse tube the flow resistance must be smaller than in an orifice pulse tube (equation (2.26)). The amplitude of the volume flow in-phase with the pressure oscillation is according to figure 2.7

$$\hat{\phi}_{\parallel} = \frac{R}{R^2 + (\omega L)^2} \hat{p}_t. \quad (2.33)$$

The phasor diagram of figure 2.7 shows that with the same imposed volume flow at the low temperature side a larger enthalpy flow can be obtained because of the smaller phase angle. It cannot be said how large the volume flow will be, because the inductance is not determined.

The optimal enthalpy flow is with equations (2.32) and (2.33)

$$\langle \dot{H} \rangle_{\text{opt}} = \frac{R_{\text{opt}}}{R_{\text{opt}}^2 + (\omega L)^2} \frac{\hat{p}_t^2}{2}. \quad (2.34)$$

With equation (2.32) and figure 2.7 it can be shown that the phase angle  $\theta_L$  would become zero if  $R = \omega L$ . The volume of the inductance is then larger than the volume of the tube. In which case the accumulation of gas in the inductance cannot be neglected. Radebaugh [10] found that one third of the capacity of the inductance must be taken into account. The presence of the inductance's capacity increases the phase angle  $\theta_L$ , as the volume flow  $\phi_H$  is ahead in phase compared to  $\phi_b$ .

### 2.4.3. Double inlet pulse tube

In the orifice and inertance pulse tube analogue we only considered that part of the cooler after the cold heat exchanger. The regenerator was not taken into account and thus also the dissipation in the regenerator not. The regenerator has a non-zero resistance  $R_r$ , resulting in a pressure drop over the regenerator. In the orifice and inertance pulse tube, the gas has to pass the regenerator to enter the pulse tube at the low temperature side. There will always be dissipation, but for a fixed volume flow the dissipation in the regenerator is constant. In the double inlet pulse tube, gas can enter the tube without first passing the regenerator via the bypass orifice,  $R_2$  in figure 2.8. In the bypass orifice there is also dissipation, as it is a pure resistance, but the sum of the dissipation in the bypass orifice and regenerator is smaller [7].

The electrical analogue, as depicted in figure 2.8, does not take temperature gradients into account. This is a shortcoming of the analogue as there is a temperature gradient over the regenerator. The volume flow at the warm side of the regenerator's resistance is at a temperature  $T_H$ , whereas the gas leaves the regenerator at a temperature  $T_L$ . The volume flow at the warm side is a factor  $T_H/T_L$  larger than the volume flow at the low temperature side of  $R_r$ .

The regenerator has not only a resistance, but also a capacity  $C_r$ . The pressure decreases from the pressure in the compressor,  $p_c$ , at the warm end of the regenerator to the pressure in the tube,  $p_t$ , at the cold end of the regenerator. The gas accumulation in the regenerator will not be at one constant pressure. In the analogue, half of the capacity is placed before the regenerator's resistance, where the accumulation is at a pressure  $p_c$ . The other half of the regenerator's capacity is placed after the resistance, where the pressure is  $p_t$ .

In the double inlet pulse tube the volume flow leaving the tube at the warm side,  $\phi_H$ , is the difference between the volume flow entering the buffer,  $\phi_b$ , and the volume flow through the bypass orifice,  $\phi_2$ .

As the bypass orifice is a pure resistance the volume flow through the bypass is

$$\hat{\phi}_2 = \frac{\hat{p}_c - \hat{p}_t}{R_2}, \quad (2.35)$$

with  $\hat{p}_c$  the pressure oscillation between the compressor and cooler. This equation together with equation (2.24) results in the following volume flow at the warm side of the tube

$$\begin{aligned} \hat{\phi}_H &= \hat{\phi}_b - \hat{\phi}_2 \\ &= \frac{\hat{p}_t}{R} - \frac{\hat{p}_c - \hat{p}_t}{R_2}. \end{aligned} \quad (2.36)$$

The volume flow at the low temperature side of the tube is the sum of the volume flow at the high temperature side of the tube and the gas accumulation in the tube

$$\hat{\phi}_L = (i\omega C_t + \frac{1}{R})\hat{p}_t - \frac{\hat{p}_c - \hat{p}_t}{R_2}. \quad (2.37)$$



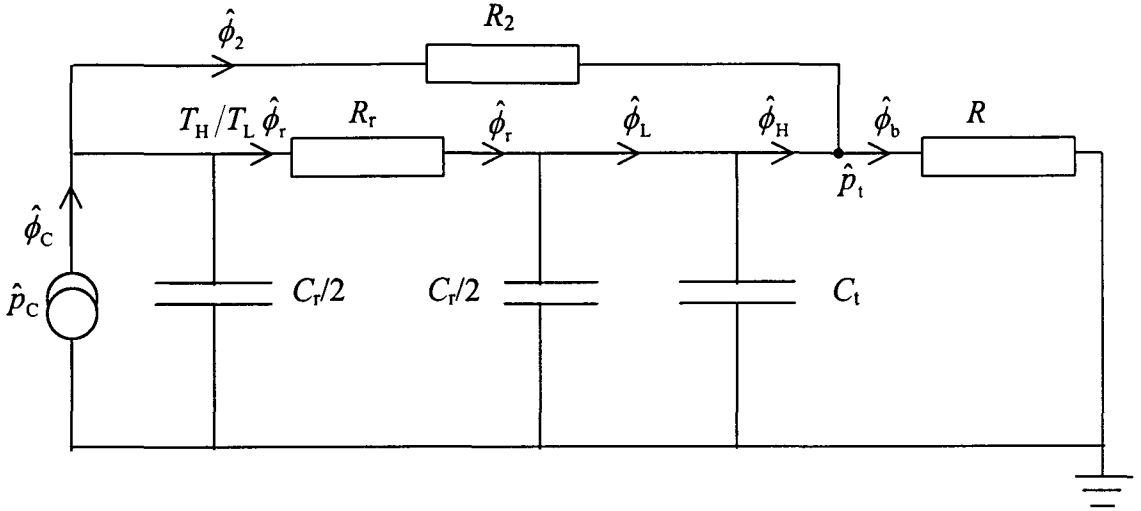


figure 2.8: Schematic overview of the double inlet pulse tube, the regenerator has a resistance  $R_r$  and capacity  $C_r$ . The bypass orifice is depicted as a resistance  $R_2$ .

The enthalpy flow in the tube can be determined if we know how the pressure in the compressor is related to the pressure in the tube. The pressure drop over the regenerator is

$$\hat{p}_c - \hat{p}_t = R_r \hat{\phi}_r, \quad (2.38)$$

while the volume flow  $\hat{\phi}_r$  is related to  $\hat{\phi}_L$  via

$$\hat{\phi}_r = i\omega(C_r/2)\hat{p}_t + \hat{\phi}_L. \quad (2.39)$$

With equations (2.37)-(2.39) the volume flow at the cold side of the tube can be expressed in terms of the present electrical components and the pressure in the tube

$$\hat{\phi}_L = \frac{i\omega(C_t - R_r/R_2(C_r/2)) + 1/R}{1 + R_r/R_2} \hat{p}_t. \quad (2.40)$$

This equation shows that the phase angle  $\theta_L$  is smaller than in an orifice pulse, see also figure 2.9. The gas in the tube is compressed in two directions: gas enters the tube from the regenerator and via the bypass orifice. The phase angle is smaller as the regenerator has a capacity in which gas accumulates, introducing a phase difference between the pressure in the tube and the compressor. Without the regenerator's capacity, the bypass orifice is still useful. With the bypass orifice, the total dissipation between the compressor and the tube decreases, increasing the pressure amplitude in the tube more than  $|\hat{\phi}_L|$  decreases.

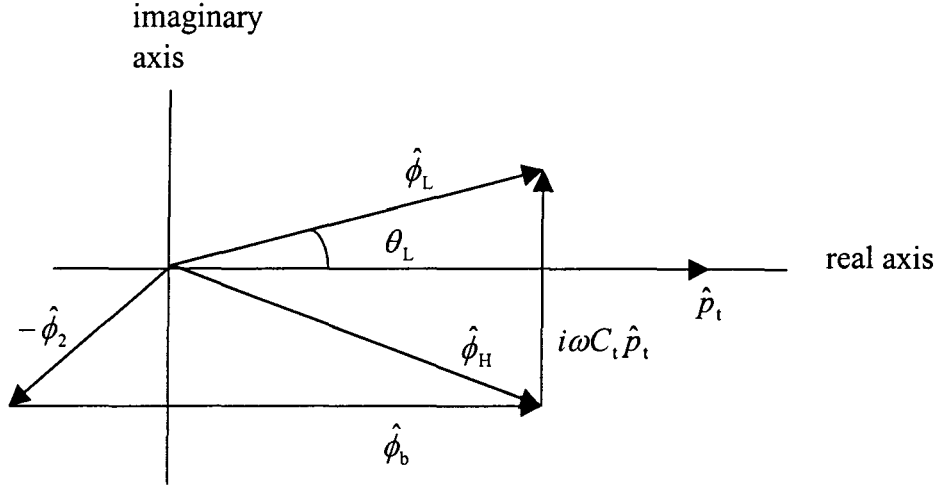


figure 2.9: Phasor diagram, illustrating the volume flows in the tube and orifices of a double inlet pulse tube cooler.

The enthalpy flow through the tube is simply

$$\begin{aligned} \langle \dot{H} \rangle &= \frac{1}{2} \text{Re}[\hat{p}_t \hat{\phi}_L^*] \\ &= \frac{1}{1 + R_r/R_2} \cdot \frac{\hat{p}_t^2}{2R}. \end{aligned} \quad (2.41)$$

To obtain a relation for the optimal bypass orifice the coefficient of performance  $\xi$  (equation (2.7)) has to be optimised. With the bypass orifice the dissipation in the regenerator decreases, but there is an additional dissipation in the orifice. We want to find a relation for  $R_2$ , for which the sum of these two dissipations is minimal. With a minimal dissipation the pressure amplitude in the tube is maximal.

The time-average work input is

$$\langle \dot{W} \rangle = \langle \hat{p}_c \hat{\phi}_c \rangle, \quad (2.42)$$

with  $\hat{\phi}_c$  the volume flow leaving the compressor. It is the sum of the volume flow through the regenerator and the volume flow through the bypass orifice

$$\begin{aligned} \hat{\phi}_c &= i\omega(C_r/2)\hat{p}_c + \frac{T_H}{T_L}\hat{\phi}_r + \hat{\phi}_2 \\ &= i\omega(C_r/2)[\hat{p}_t + R_r\hat{\phi}_r] + \left[\frac{T_H}{T_L} + \frac{R_r}{R_2}\right]\hat{\phi}_r. \end{aligned} \quad (2.43)$$

With equations (2.39) and (2.40) the volume flow  $\hat{\phi}_r$  becomes

$$\hat{\phi}_r = \frac{i\omega((C_r/2) + C_t) + 1/R}{1 + R_r/R_2} \hat{p}_t. \quad (2.44)$$

Resulting in the following equation

$$\langle \dot{W} \rangle = \left( \frac{T_H}{T_L} + \frac{R_r}{R_2} \right) \left\{ 1 + \frac{R_r/R}{1 + R_r/R_2} [(\omega R)^2 (C_t + (C_r/2))^2 + 1] \right\} \cdot \frac{\hat{p}_t^2 / 2R}{1 + R_r/R_2}. \quad (2.45)$$

The time-average work flow is proportional to the enthalpy flow through the tube (equation (2.41)). The enthalpy flow is (in the ideal case) equal to the cooling power, so the coefficient of performance is the ratio of equation (2.41) and equation (2.45)

$$\xi = \frac{1}{\left( \frac{T_H}{T_L} + \frac{R_r}{R_2} \right) \left\{ 1 + \frac{R_r/R}{1 + R_r/R_2} [(\omega R)^2 (C_t + (C_r/2))^2 + 1] \right\}}. \quad (2.46)$$

It can be shown by differentiation of equation (2.46) to  $R_2$  that the performance is maximal if

$$R_{2,\text{opt}} = \frac{R_r}{-1 + \sqrt{\xi_{\text{car}}^{-1} \frac{R_r}{R} [(\omega R)^2 (C_t + (C_r/2))^2 + 1]}}, \quad (2.47)$$

with  $\xi_{\text{car}} = T_L / (T_H - T_L)$  the Carnot coefficient of performance.

Differentiation to  $R$  of equation (2.46) results in following optimum for the orifice between buffer and tube

$$R_{\text{opt}} = \frac{1}{\omega (C_t + (C_r/2))}. \quad (2.48)$$

This equation differs from equation (2.26), because in the single orifice pulse tube analogue we did not take the capacity of the regenerator into account. If it is not neglected the optimal phase angle lowers in value [11]. The equation shows that the optimal orifice is independent of the bypass orifice.

Substitution of the optimal orifice in equation (2.47) gives

$$R_{2,\text{opt}} = \frac{R_r}{-1 + \sqrt{2\xi_{\text{car}}^{-1} \omega R_r (C_t + (C_r/2))}}. \quad (2.49)$$

If the regenerator's resistance and capacity is known, together with the temperature of the low temperature and high temperature side of the regenerator the optimal bypass orifice can be calculated.

## 2.5 Enthalpy flow through an adiabatic tube with a thermal boundary layer

Until now the gas in the tube is considered completely adiabatic. Which means that there is an oscillating temperature  $\hat{T}$  related via Poisson's relation to the oscillating pressure  $\hat{p}$

$$\hat{T} = \frac{\hat{p}}{c_p \rho_0}. \quad (2.50)$$

However, in reality there is always some interaction between gas and wall, which modifies the oscillating temperature in the boundary layer. In this section this modification is deduced in terms of the gas's distance from the centre of the tube:  $T(x,r)=T_0(x)+\hat{T}(x,r)e^{i\omega t}$ . The distance over which the fluid temperature is influenced by the wall is roughly equal to the thermal penetration depth [8]

$$\delta_T = \sqrt{\frac{2\lambda}{c_p \omega \rho_0}}. \quad (2.51)$$

The thermal penetration depth is the distance over which heat can diffuse through the fluid, during a time  $1/\omega$ . In this equation is  $\lambda$  the heat conduction coefficient.

The wall temperature is assumed constant in time, with a constant temperature gradient  $\nabla T_0$ . The heat conduction coefficient is taken to be temperature independent and axial conduction in the gas is neglected.

With all these simplifications, the resulting energy equation becomes [8]:

$$\rho T \frac{ds}{dt} = \lambda \nabla^2 T, \quad (2.52)$$

with  $s$  the specific entropy of the fluid.

To express the change in entropy in terms of a change in temperature and pressure, we substitute the following combination of first and second law for reversible processes in equation (2.52) [6]

$$Tds = c_p dT - \frac{1}{\rho} dp. \quad (2.53)$$

This results in a differential equation for the unknown oscillating temperature in terms of the known pressure and velocity oscillation and wall temperature gradient

$$c_p \rho_0 (i\omega \hat{T} + \hat{u} \nabla T_0) - i\omega \hat{p} = \lambda \left( \frac{1}{r} \frac{\partial \hat{T}}{\partial r} + \frac{\partial^2 \hat{T}}{\partial r^2} \right). \quad (2.54)$$

The equation is solved with the boundary conditions that there is no temperature oscillation at the wall,  $r=R_t$  and the oscillation is finite at the centre of the tube,  $r=0$  [12]:

$$\hat{T}(r) = \left( \frac{\hat{p}}{c_p \rho_0} - \frac{\hat{u} \nabla T_0}{i\omega} \right) (1 - e^{-(1+i)\chi(R_t-r)/\delta_T}). \quad (2.55)$$

As  $\delta_T \ll R_t$ , the gas near the centre of the tube makes negligible thermal contact with the wall. The exponential term vanishes. The remaining equation describes the behaviour of an adiabatic gas. The first term is equal to equation (2.50): temperature variation due to adiabatic compression and expansion. The second term is due to the temperature gradient in the gas. The actual temperature oscillation is a linear superposition of these two effects. A given piece of gas increases in temperature due to the adiabatic compression, but at the same time it moves along the positive  $x$  axis where there is a higher mean temperature.

If the rise in temperature due to compression exactly equals the temperature increase due to displacement, we speak of a critical temperature gradient defined as:

$$\nabla T_{\text{crit}} \equiv \frac{\omega |\hat{p}|}{c_p \rho_0 |\hat{u}|}. \quad (2.56)$$

In this situation the temperature at a given location remains constant in time. In a basic pulse tube the critical temperature gradient determines the low temperature limit. If the temperature rise of the gas equals the increase in temperature of the wall due to the displacement of the gas, there will be no heat exchange between the gas and the surface. In an orifice pulse tube the temperature gradient of the wall is generally larger than the critical temperature gradient. In this situation the compressed gas near the wall will absorb heat and transfer it to the cold side, where the heat is rejected to the surface. To lower this heat flow from the warm to the cold side, the displacement of the gas must be decreased. This is the case in the double inlet pulse tube and the inertance pulse tube, where the gas is compressed from two sides.

The critical temperature gradient is at the cold side of the tube smaller than at the warm side, as the displacement of the gas is dependent of the axial position in the tube. At the low temperature side, the velocity is larger than at the high temperature side as can be seen in equation (2.19), while the pressure amplitude is constant throughout the tube.

The total enthalpy flow at a cross-section of the tube can be calculated if equation (2.50) is substituted in equation (2.14)

$$\begin{aligned} \langle \dot{H} \rangle &= c_p \rho_0 \int_{A_t} \langle \hat{u} \hat{T} \rangle dA \\ &= \frac{1}{2} c_p \rho_0 \int_{A_t} \text{Re}[\hat{u} \hat{T}^*] dA. \end{aligned} \quad (2.57)$$

The oscillatory velocity is written as the sum of a real and an imaginary part,  $\hat{u} = \hat{u}_{\text{re}} + i\hat{u}_{\text{im}}$ . Together with the oscillating temperature of equation (2.55), the enthalpy flow is approximately

$$\langle \dot{H} \rangle = \frac{1}{2} \pi |\hat{p}| \cdot [\hat{u}_{\text{re}} (R_t^2 - \delta_T R_t) + \hat{u}_{\text{im}} \delta_T R_t - |\hat{u}|^2 \frac{c_p \rho_0}{\omega |\hat{p}|} \nabla T_0 \delta_T R_t]. \quad (2.58)$$

The total enthalpy flow is the sum of three components: the adiabatic enthalpy flow, surface heat pumping and the gradient effect:

$$\begin{aligned} \langle \dot{H}_{\text{ad}} \rangle &= \frac{1}{2} |\hat{p}| \|\hat{\phi}\| \cos \theta \cdot \left(1 - \frac{\delta_T}{R_t}\right), \\ \langle \dot{H}_{\text{su}} \rangle &= \frac{1}{2} |\hat{p}| \|\hat{\phi}\| \sin \theta \cdot \frac{\delta_T}{R_t}, \\ \langle \dot{H}_{\text{gr}} \rangle &= -\frac{1}{2} \|\hat{\phi}\|^2 \cdot \frac{c_p \rho_0}{\omega A_t} \nabla T_0 \frac{\delta_T}{R_t}. \end{aligned} \quad (2.59)$$

The first component is the adiabatic enthalpy flow as calculated in section 2.3, but now modified for a tube with a (small) thermal boundary layer. If there would be no thermal penetration, the only remaining term would be this adiabatic enthalpy flow. Surface heat pumping is the only cooling mechanism in the basic pulse tube as there the volume flow

has only an out-of-phase component with the pressure amplitude. In the surface heat pumping component, the temperature gradient is not taken into account. Surface heat pumping is the product of the pressure oscillation and the out-of-phase volume flow, while the displacement of the gas has both an out-of-phase and an in-phase component. This results in an extra negative component, the gradient effect, as there is a positive mean temperature gradient over the tube's length.

# Chapter 3

## The experimental apparatus

In this chapter the experimental apparatus will be discussed. First a brief review of the pulse tube refrigerator will be given and some parts of the cooler will be discussed in detail. After that, the measuring devices will be discussed and in the third section the orifices will be characterized.

Two pulse tube refrigerators have been used, for the greatest part the same, but with some important differences. In section 3.1 there is also a table with an overview of the two coolers.

### 3.1 Refrigeration system

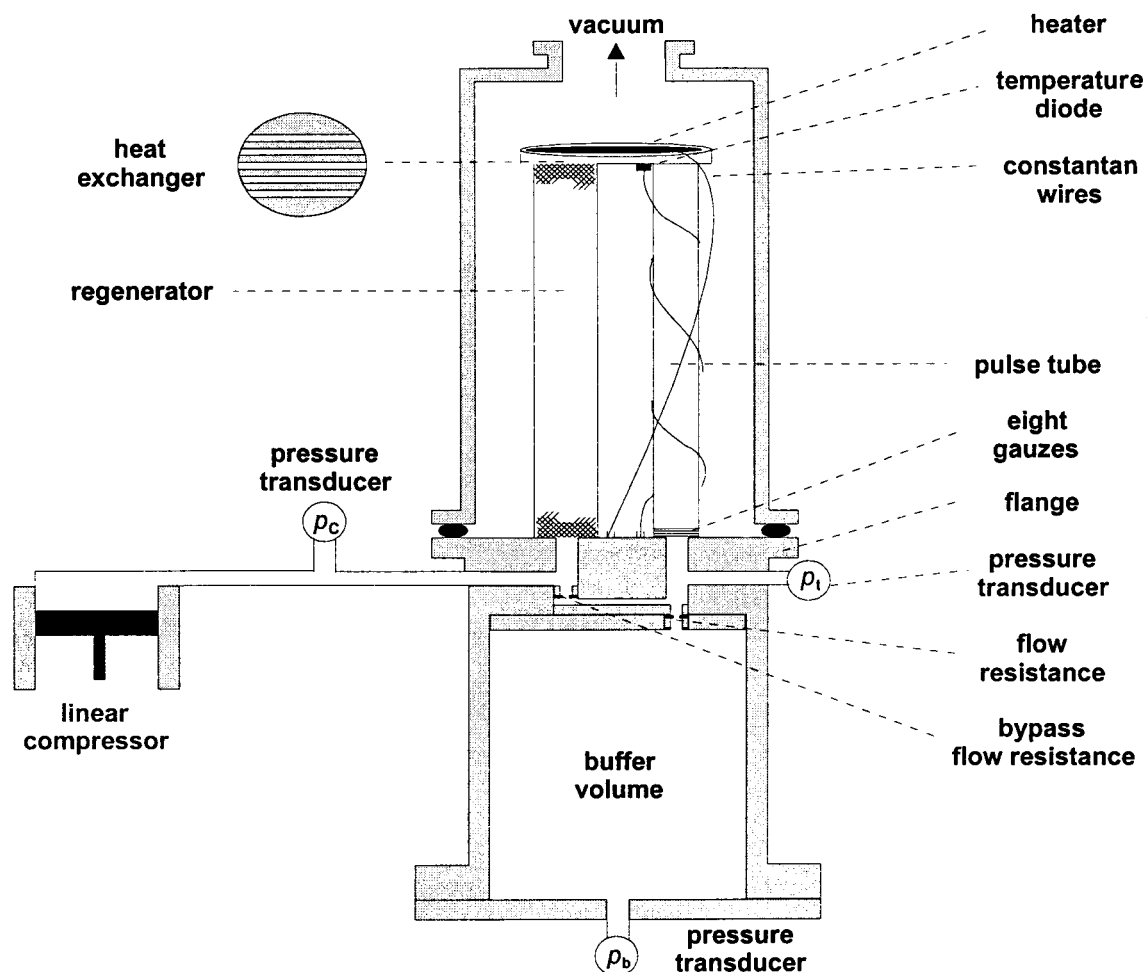


*figure 3.1: Schematics of the pulse tube refrigerator used for the experiments.*

Until now, the cooler has been depicted as an apparatus with the cold heat exchanger in the middle. In practice, the cooler will be used to cool some device, so it is more practical to have the cold heat exchanger at the top so it can be easily attached. This is

the reason why the cooler as depicted in figure 3.1 is U-shaped with a flat cold heat exchanger surface at the top.

The refrigeration system as depicted in figure 3.1 consist of a compressor, regenerator, pulse tube, buffer volume, cold heat exchanger, (secondary) flow resistance and connecting tubes. For all experiments, the working gas was helium.

The compressor is a one piston linear compressor with a diameter of 15 mm. Two pulse tube coolers are used, one with the regenerator and pulse tube 55 mm long and in the other, both are 70 mm long. The regenerator is a stainless steel tube with an internal diameter of 8.77 mm and a wall thickness of 0.15 mm. The regenerator is filled with stainless steel gauzes. The 55 mm regenerator with gauzes of a mesh of 180 and a wire diameter of 35  $\mu\text{m}$ , the 70 mm regenerator with a mesh of 325 and a wire diameter of 23  $\mu\text{m}$ , see also section 3.1.1. The pulse tube is also a stainless steel tube with an internal diameter of 6.1 mm and a wall thickness of 0.15 mm. The warm end of the tube contains eight gauzes for flow straightening. The cold heat exchanger is a stainless steel flat disc with five channels each 1 mm wide and spaced 1 mm from each other. There are no real heat exchangers at the warm ends of tube and regenerator, the eight gauzes at the warm end of the tube and the connecting tubes to buffer volume or compressor have to be sufficient. The buffer has a volume of 37  $\text{cm}^3$  and can be extended when a long inertance is used, see section 3.1.2.

The regenerator, pulse tube and cold heat exchanger are placed in a cylindrical vacuum vessel. In the vessel a pressure of  $10^{-5}$ - $10^{-6}$  mbar is maintained to lower the thermal radiation from the environment. Further improvement is obtained with a radiation screen of mylar that surrounds the regenerator and tube. The pulse tube refrigerator is mounted on a water-cooled table (18  $^{\circ}\text{C}$ ) with the aid of a heat sink.

table 3.1: Overview of the two refrigerators.

<b>pulse tube cooler</b>	<b>55 mm</b>	<b>70 mm</b>
tube length $L_t$ [mm]	55	70
cross-section $A_t$ [ $\text{mm}^2$ ]	29	29
length regenerator $L_r$ [mm]	55	70
cross-section $A_r$ [ $\text{mm}^2$ ]	60	60
number of gauzes $n$ [-]	850	1850
mesh [ $\text{inch}^{-1}$ ]	180	325
wire diameter $d_d$ [ $\mu\text{m}$ ]	35	23
filling factor $f$ [-]	0.22	0.29

### 3.1.1. The regenerator

The regenerator is filled with stainless steel gauzes. These gauzes are woven as depicted in figure 3.2. The gauzes are normally characterized by their mesh number, which is the number of wires per inch in one direction and their wire diameter  $d_d$ . From these numbers the filling factor  $f$  of the regenerator can be calculated

$$f = \frac{\pi d_d}{4t} \sqrt{1 + \frac{d_d^2}{t^2} \frac{2nd_d}{L_r}}. \quad (3.1)$$



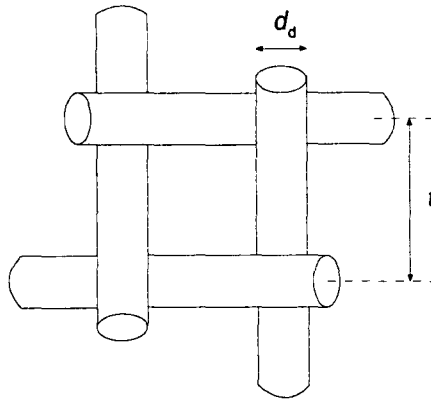


figure 3.2: Geometry of gauzes.

In this equation is  $t$  the average distance between two wires,  $n$  the number of gauzes and  $L_r$  the length of the regenerator.

An ideal regenerator imposes locally isothermal conditions on the gas and has no flow resistance. To impose locally isothermal conditions, the regenerator must have a high heat capacity, a good heat exchange surface and no axial heat conduction. With these three conditions it absorbs (or rejects) heat from (to) the gas without increasing in temperature. The heat capacity is proportional to the filling factor as is also the heat exchange surface. This implies that the regenerator should have a filling factor as high as possible. A regenerator with a filling factor as low as possible has a small flow resistance, resulting in a small pressure drop over the regenerator. With a low filling factor, the axial conduction through the regenerator is small, as the mutual contact of the gauzes is small. The mass flow arriving at the cold side is smaller than at the warm side as the amount of void volume in the regenerator is large.

An example: two regenerators with the same length and diameter, the first with a small filling factor and the second with a filling factor near one. In both situations the same input power to the compressor is applied. With a small filling factor the mass flow at the warm side is higher than at the cold side, but as the resistance is small the mass flow is large and thus also the pressure amplitude in the tube. With a high filling factor the mass flow through the regenerator is almost constant, but as the resistance is high the mass flow is small and thus also the pressure amplitude in the tube. The resulting enthalpy flow through the pulse tube will be higher for the first situation (see for example equation (2.21)), with a low filling factor. In an ideal pulse tube refrigerator the cooling power is equal to this enthalpy flow. With a non-ideal regenerator, there is an enthalpy flow and heat conduction in the regenerator to the cold heat exchanger. The amount of enthalpy that arrives at the cold heat exchanger is dependent on the filling factor. In the first regenerator, with the low filling factor, a larger amount of enthalpy will reach the cold heat exchanger. On the other hand, the heat conduction through the gauzes is small in the first regenerator. The net cooling power is the difference between the enthalpy flow in the tube and the sum of the enthalpy flow and heat conduction in the regenerator. The aim is to find an optimum between: heat capacity, heat exchange surface, pressure drop, mass flow and heat conduction.

The diameter of the regenerator is larger than the diameter of the pulse tube. With the larger diameter the regenerator has enough heat exchange surface and heat capacity to store this heat and still have enough empty space so that the pressure drop and heat conduction are small.

### 3.1.2. Orifices and inertances

The pulse tube has been constructed in such a way that the flow resistance (orifice or inertance) and bypass orifice are easily replaced via the buffer volume. The flow resistance is laid in a plate and sealed with a rubber O-ring. This plate is attached to the flange with screws.

The orifices are round flat stainless steel discs with an external diameter of 4 mm and thickness 0.25 mm. In the middle, the orifices have a hole with a diameter between 0.15 mm and 0.4 mm.

The inertances are soft copper capillaries with an internal diameter of 0.79 mm, 0.91 mm, 1.02 mm or 1.32 mm and variable length. The internal diameter has a tolerance of  $\pm 0.03$  mm. The beginning of the inertance is laid in the plate and the remaining is wound in the buffer volume. To make this possible the buffer volume is enlarged in some cases.

## 3.2 Measuring system

The measurement system [13] includes devices to measure the pressure, the temperature and the net cooling power. In addition, the mechanical input power delivered by the compressor is measured as is also the piston stroke.

Three pressure transducers measure the mean and oscillating pressure. The transducers are mounted in the connection tube between compressor and regenerator, in the pulse tube at the warm end and in the buffer. The pressure transducers are based on a piezoelectric element with a dynamic range from 0 to 2000 Hz. The transducer returns an output voltage depending on the resistance of the piezo-resistive element. The output signal is amplified and to lower the noise the oscillating component is averaged. A temperature diode attached to the bottom of the cold heat exchanger measures the low temperature. At the top of the cold heat exchanger a heater is glued to apply the cooling power. The piston stroke is measured with an LVDT (Linear Variable Differential Transformer). The LVDT is an electromechanical transducer. To measure the position of the piston a metal rod is attached to the back of the piston, the rod moves in the LVDT.

The set-up is controlled with a personal computer. A Turbo Pascal program calculates and controls the mechanical input power to the compressor and its frequency. The temperature of the cold heat exchanger can be fixed. The program controls the temperature and applies heat to the cold heat exchanger when necessary.

In all experiments the amount of energy put in the piston of the compressor, the mechanical input power is kept constant. The electrical input power to the compressor is higher. The difference is due to energy losses in the wire of the compressor's coil. The compressor has a resonance frequency of 42 Hz, if the 55 mm pulse tube cooler is used and the mean pressure is 1.6 MPa. When the compressor is used off-resonance the electrical input power to the compressor must increase, to maintain the same mechanical input power.

### 3.3 Characterization of the orifices

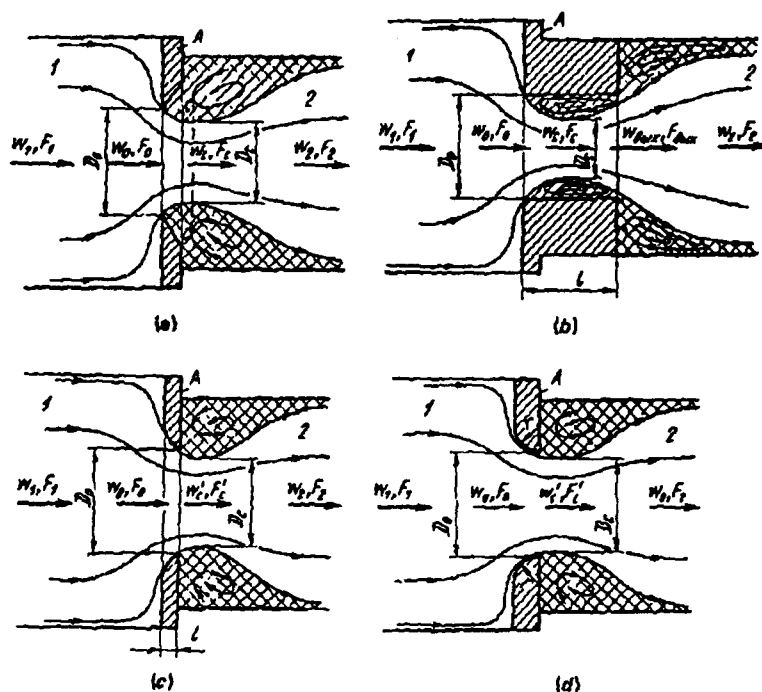


figure 3.3: General case of flow passage through an orifice in the wall from one volume into another: (a) sharp-edged orifice; (b) orifice with thick edges; (c) orifice with edges beveled in the flow direction; (d) orifice with edges rounded in the flow direction. (copied from [14])

The orifice serves as a flow resistance. The orifices are thin plates with abrupt transitions. In an abruptly expanded cross-section a jet is formed. Vortices develop and gradually disappear while the emerging jet completely spreads over the cross-section. When a fluid passes an orifice, the fluid jet is somewhat smaller than the hole itself. This constriction is called the vena contracta. The passage of the orifice is accompanied by a distortion of the trajectories of the particles with the result that they continue their motion towards the axis of the orifice. The size of the fluid jet emerging is dependent of the orifice shape, see figure 3.3 [14]. If the fluid passes an orifice with sharp edges (see figure 3.3a) the jet emerging is smallest (cross-section  $F_c$ ). A thicker orifice (figure 3.3b), an orifice with edges beveled in the flow direction (figure 3.3c) or an orifice with rounded edges (figure 3.3d) has a larger jet (cross-section  $F_c' > F_c$ ). As the cross-section of the jet emerging is larger the resistance of the orifice decreases.

Steady flow measurements have been done in order to characterize the different orifices. Orifices with various hole diameters have been tested. For these measurements the pulse tube is disconnected from the compressor and connected to a bottle of helium. The helium gas flows from the bottle through the pulse tube and orifice into the surroundings. Between the bottle and the pulse tube, a flow-controlling valve and a flow meter are mounted. The pressure before the orifice is measured with the pressure

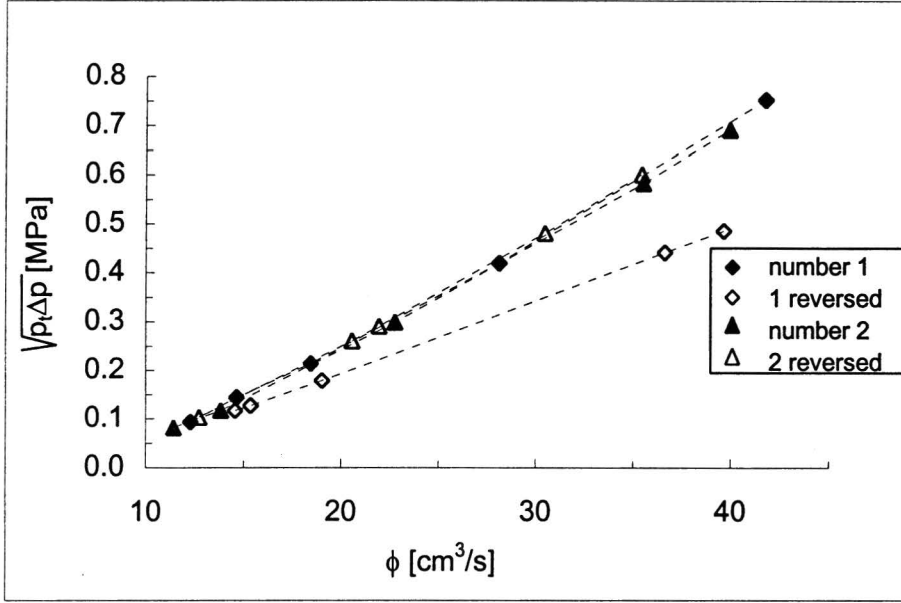


figure 3.4: Measured pressure difference versus volume flow for two orifices with a diameter of 0.15 mm.

transducer of the pulse tube and after the orifice the pressure is equal to the atmospheric pressure.

The loss in pressure can in this case be formulated as [14]

$$\Delta p_{\text{diss}} = p_t - p_{\text{air}} = \zeta \cdot \frac{1}{2} \rho_t u_t^2, \quad (3.2)$$

with  $\zeta$  the friction coefficient of the orifice.

The flow meter measures the volume flow  $\phi_{\text{flow}}$  for standard conditions, but the flow through the tube is at another, higher pressure:

$$\phi_{\text{flow}} = \frac{p_t}{p_{\text{air}}} \phi_t = \frac{p_t}{p_{\text{air}}} A_t u_t. \quad (3.3)$$

Equations (3.2) and (3.3) together with the equation of state for an ideal gas gives:

$$\phi_{\text{flow}} = \sqrt{\frac{2A_t^2 R_m T}{\zeta p_{\text{air}}^2}} \cdot \sqrt{p_t \Delta p}. \quad (3.4)$$

The first square root on the right side represents the conductivity of the orifice, which is proportional to the reciprocal of the flow resistance of the orifice. The flow resistance  $R$  of the orifice is defined at standard air pressure:

$$R \equiv \frac{\sqrt{p_t \Delta p}}{\phi_{\text{flow}}}. \quad (3.5)$$

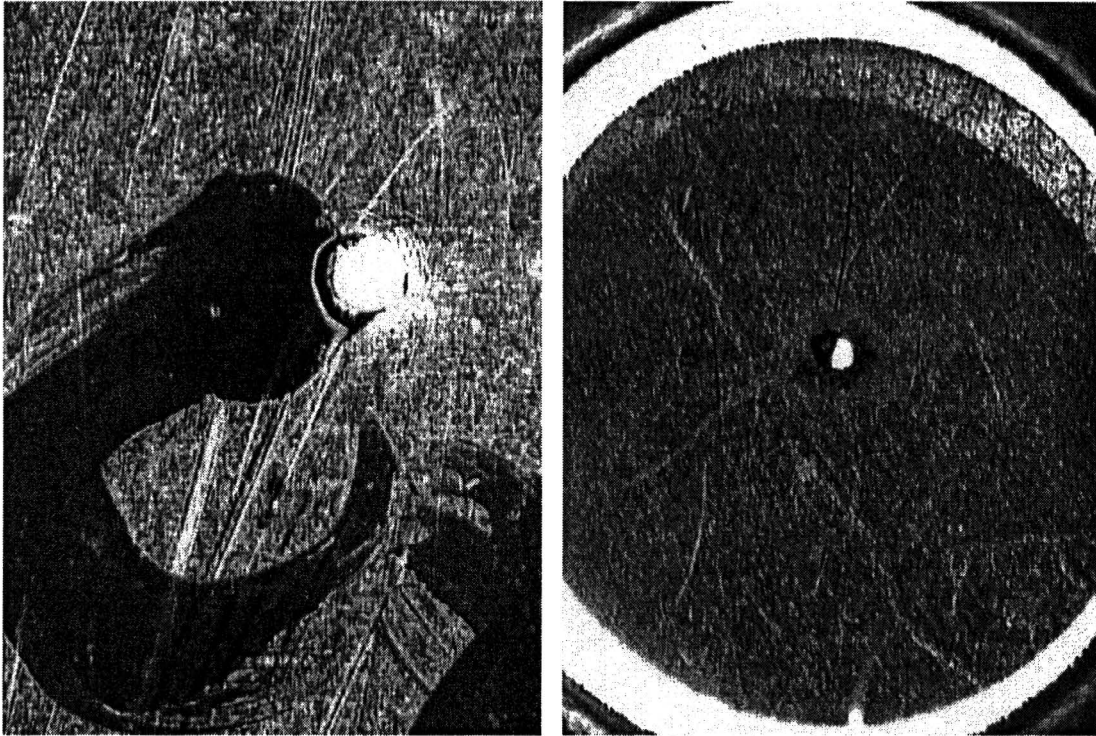


*figure 3.5: Photo of a drilled orifice (left) and one shot with a laser (right).*

Some holes are drilled which leaves a burr at one side of the orifice as can be seen on the left photo in figure 3.5. Without the burr, the edges of the hole should be straight. With a burr at one side the orifices are not symmetric. This results in flow resistances that can differ quite a lot when turned around, see figure 3.4.

There are also some measurements done with holes shot with a laser at the University of Twente. These orifices have symmetric flow resistances as can be seen in figure 3.6 where they are depicted as triangles. The disadvantage of these orifices is that the diameter is not exactly known. The material on the place where the hole has to come melts and flows down, where it solidifies. The resulting holes are not completely round as can be seen on the right photo of figure 3.5. The aim was to make orifices with a diameter between 0.15 and 0.2 mm, but due to the highest resistances measured it is probable that the effective diameter is smaller.

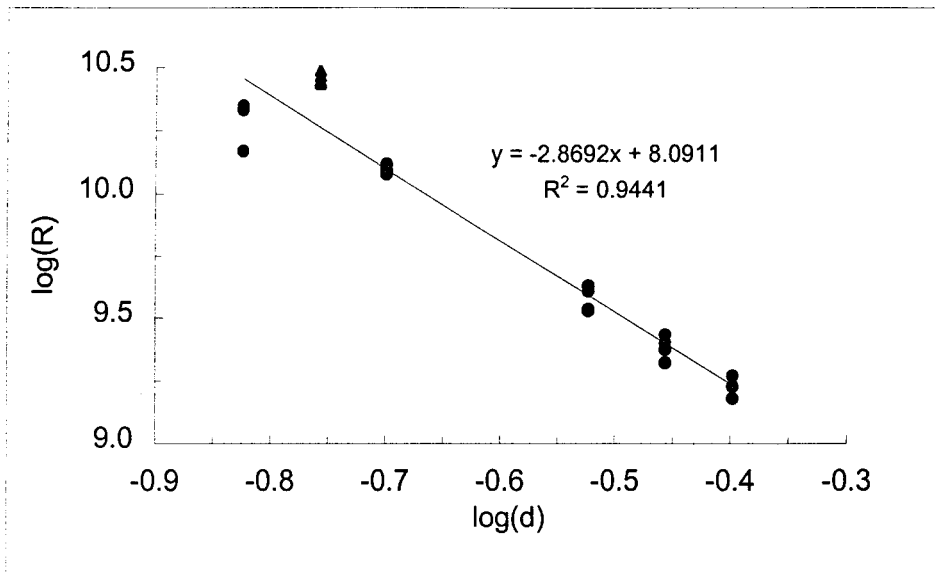


figure 3.6: Resistance measurements of orifices with a diameter varying between 0.15 and 0.4 mm.

It is assumed that there is some kind of relation between the flow resistance and the diameter [mm] of the form:

$$R = \frac{a}{d^\alpha}, \quad (3.6)$$

with  $a$  and  $\alpha$  to determine constants.

Flow measurements have been done with drilled orifices with diameters of 0.15, 0.2, 0.3, 0.35 and 0.4 mm (depicted as circles in figure 3.6) and with the shot orifices. In figure 3.6 both the flow resistance and the diameter are plotted on a logarithmic scale:

$$\begin{aligned} {}^{10}\log(R) &= {}^{10}\log(a) - \alpha {}^{10}\log(d), \\ &\text{with } \alpha = 2.9, \\ &{}^{10}\log(a) = 8. \end{aligned} \quad (3.7)$$

So the flow resistance of the orifices is likely to be proportional to  $d^{-3}$ .

# Chapter 4

## The 55 mm pulse tube cooler

In this chapter the performance of the pulse tube cooler will be examined in which the regenerator and pulse tube both are 55 mm long. The first experiments have been done with an orifice pulse tube. Three orifice diameters have been used. The results of these experiments will be discussed in section 4.1. The following experiments have been done with an inertance pulse tube. Three different inertance diameters have been used. Each inertance has been varied in length in order to find the optimum length. The results with an inertance pulse tube will be discussed in section 4.2. The few experiments that have been done with a double inlet pulse tube will be discussed in section 4.3.

### 4.1 The orifice pulse tube

The orifices used in the experiments are the same as the ones used in the steady flow measurements. In the steady flow experiments, the gas flow through the orifice was in one direction, while in a pulse tube the gas flows back and forth.

For an oscillating flow, equation (3.5) can be divided in two components. One component describing the amount of gas leaving the tube, the volume flow leaving the tube entering the buffer volume,  $\phi_{t \rightarrow b}$ . The other component describing the amount of gas entering the tube, the volume flow from buffer to tube,  $\phi_{b \rightarrow t}$ :

$$\begin{aligned}\phi_{t \rightarrow b} &= \frac{\sqrt{p_t |\Delta p|}}{R_{t \rightarrow b}}, \\ \phi_{b \rightarrow t} &= \frac{\sqrt{p_b |\Delta p|}}{R_{b \rightarrow t}}.\end{aligned}\tag{4.1}$$

If the resistance of the orifice is the same in both directions,  $R_{t \rightarrow b} = R_{b \rightarrow t}$ , the amount of gas leaving the tube will be larger than the amount of gas that enters the tube. This is due to the higher pressure amplitude in the tube:  $p_{t(b)} = p_0 + |\hat{p}_{t(b)}|$ . Because of this the mean pressure in the buffer will increase, during operation, until an equilibrium is reached. In section 3.3, the flow measurements showed that the resistance was not always the same in both directions. Although a different mean pressure in tube and buffer has no consequence for the operation of the cooler, it is tried to obtain the same mean pressure in both tube and buffer. The orifice is put in the cooler in such a way that the resistance from tube to buffer is larger than the resistance from buffer to tube.

In the experiments, however, the measured mean pressure in the tube was almost always slightly higher than the mean pressure in the buffer volume. This is probably because the pressure oscillations are not perfectly sinusoidal. The pressure increase is larger than the pressure decrease. The compressor compresses all the gas in the cooler. Some is compressed isothermally and some adiabatic. There are also temperature differences in the refrigerator, the volume is corrected for these temperature variation via  $V_0 = \sum V_i (T_H / T_i)$ . The regenerator has a flow resistance and at the warm end of the tube

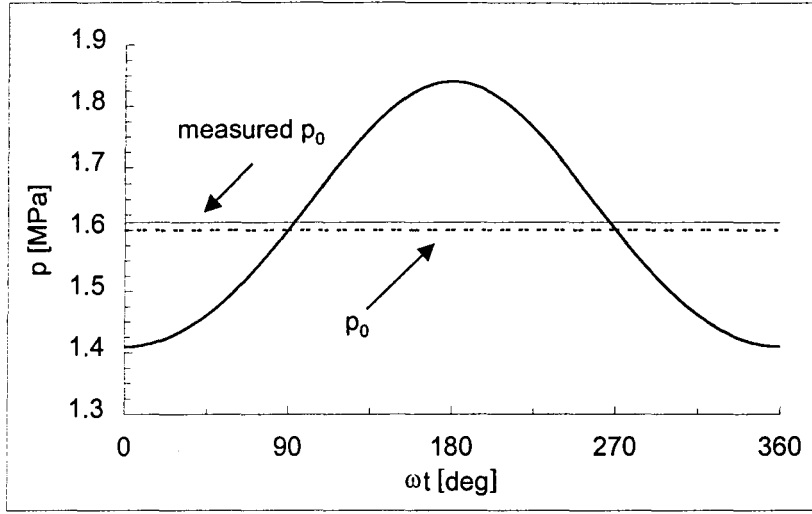


figure 4.1: Pressure oscillation in the tube. In this example is  $|\hat{V}|=1.2$   $cm^3$ ,  $V_0=12 cm^3$  and  $\alpha=1.33$ .

gas is leaving the tube. All this makes it impossible to find an exact equation for the pressure in the cooler. For stirling coolers there is a correction factor applied for the isothermal/adiabatic ratio. Here we use  $\alpha=1.33$ , the average of isothermal ( $\alpha=1$ ) and adiabatic compression ( $\alpha=\gamma=1.67$ ). With a sinusoidal piston motion the sum of the mean and oscillating pressure is written as

$$p = \frac{mR_m T}{(V_0 + \hat{V} \cos \omega t)^\alpha}, \quad (4.2)$$

with  $V_0$  the volume before the piston and  $|\hat{V}|$  the volume change caused by the motion of the piston.

In this situation the pressure increases more than it decreases, see figure 4.1. The oscillating pressure is not sinusoidal, although the piston motion is. In the example depicted in figure 4.1 the measured time averaged mean pressure  $p_0=1.613$  MPa, slightly higher than  $p_0$ . In this example the ratio of the pressure amplitude and mean pressure  $|\hat{p}|/p_0 = 0.14$ , while in the experiments with this cooler, the ratio can be up to 0.25 increasing the difference a bit more.

With an oscillating flow, the measured orifice resistance is not the same as in the steady flow measurements. The resistance of an orifice in steady flow measurements is around three times higher than the resistance of the same orifice in a pulse tube, with oscillation frequencies between 30 and 50 Hz. This was also noticed in previous experiments done at Signaal USFA. The reason for this is not exactly known. One of the reasons is probably that the steady flow measurements are done at other Reynolds numbers. In the tube, Reynolds number was between 20 and 800 during the flow measurements. In the working pulse tube the peak Reynolds number was around 1000.

In section 2.4 it was deduced that an ideal pulse tube reaches optimal performance if the flow resistance  $R_{opt}=1/\omega C_t$ . Together with equation (3.7) and the assumption that the resistance in an oscillating flow is three times smaller than the steady flow resistance, the optimal orifice diameter can be calculated. For frequencies  $f$ , with  $f=\omega/2\pi$ , around



40 Hz an orifice diameter of 0.45 mm should give the best results. This optimum is calculated for a fixed volume flow  $|\hat{\phi}_L|$ . The dissipation in the regenerator is in this situation constant. In reality the dissipation in the regenerator is dependent on the filling factor and length of the regenerator. If the regenerator is taken into account it can be shown that for a filling factor smaller than one and with a regenerator resistance, the optimum is at a phase angle somewhat smaller than  $45^\circ$  [11]. A smaller phase angle is obtained if the orifice resistance is smaller and thus the orifice diameter larger.

### Measurements

Experiments with two orifices at three different frequencies are done and with an orifice diameter of 0.3 mm at a frequency of 40 Hz. The mean pressure during the experiments was 1.6 MPa and the mechanical input power 20 W.

As can be seen in figure 4.2 the lowest temperature reached is 110.5 K. This temperature is reached with an orifice diameter of 0.35 mm at a frequency of 35 Hz. The best performing orifice is frequency dependent. As the frequency increases the best performing orifice diameter increases. For a frequency of 35 Hz the low temperature difference is 3 K between the 0.35 mm and 0.4 mm orifice diameter orifice. With a frequency of 40 Hz, the low temperature difference decreases to less than 1 K between the two orifice diameters. With  $f=45$  Hz the largest orifice diameter,  $d=0.4$  mm, reaches the lowest temperature.

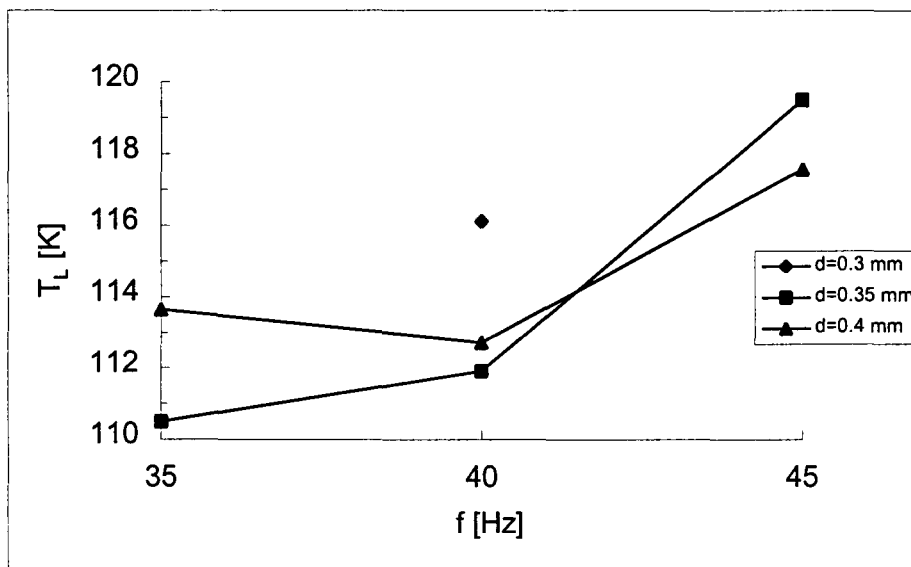


figure 4.2: Minimum temperature of the cold heat exchanger versus frequency. Three orifice diameters are tested. The mechanical input power was 20 W and the mean pressure 1.6 MPa.

The cooling power at a fixed cold heat exchanger temperature,  $T_L$ , is determined. The amount of heat required to keep the temperature constant is the cooling power. In figure 4.3, the results with an orifice diameter of 0.35 mm are depicted. The figure shows that the cooling power increases linear with  $T_L$ . The lines for the three frequencies are approximately parallel. The slope of the lines increases slightly with an increasing frequency. The difference is the minimum low temperature. With a frequency of 35 Hz the lowest temperature is reached and consequently the cooling power in the measured temperature range is the highest.

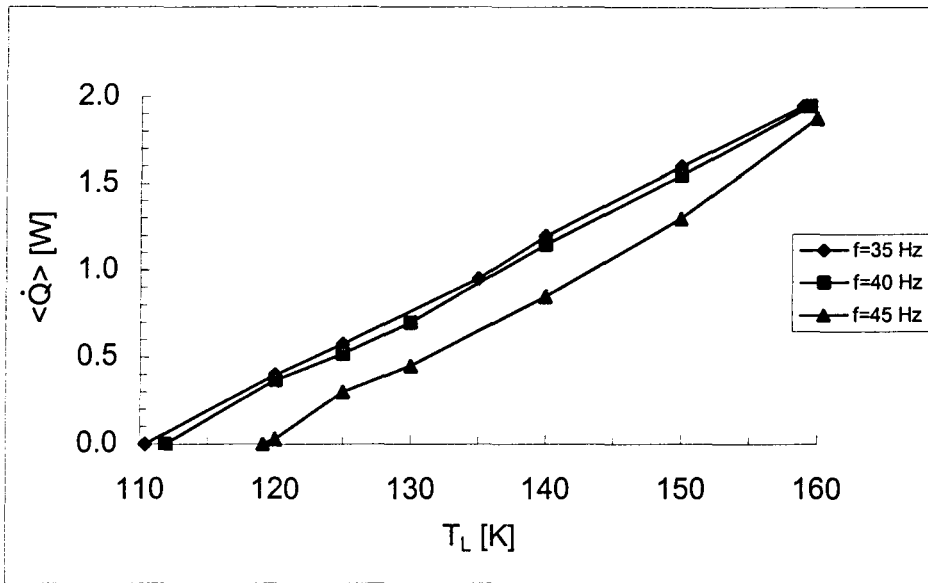


figure 4.3: Cooling power versus cold heat exchanger temperature with an orifice diameter of 0.35 mm. The mean pressure was 1.6 MPa and the mechanical input power 20 W.

As the cooling power increases linear with  $T_L$ , it is possible to determine one, constant slope for the measured temperature interval. The slope is called the cooling power per kelvin. Together with the minimum cold heat exchanger temperature, it determines the performance of the cooler at a certain low temperature.

In figure 4.4, the cooling power per kelvin versus the frequency is depicted for three orifice diameters. The cooling power per kelvin increases if the orifice diameter increases. With an orifice diameter of 0.35 mm the cooling power per kelvin increases with an increasing frequency, while with a 0.4 mm orifice it has a maximum at a frequency of 40 Hz. The highest cooling power per kelvin measured is with the 0.4 mm orifice at a frequency of 40 Hz:  $\Delta\langle\dot{Q}\rangle/\Delta T_L = 47$  mW/K.

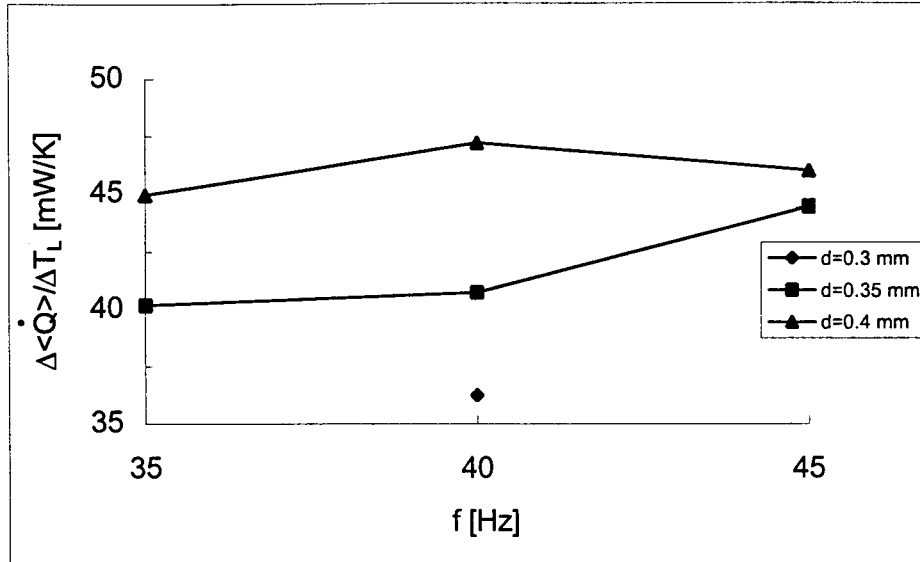


figure 4.4: Average cooling power per kelvin versus frequency for three orifice diameters. All measurements are done with a mean pressure of 1.6 MPa and a mechanical input power of 20 W.

### Discussion

The best performing orifice diameter is 0.35 mm, this is smaller than the calculated optimum ( $\theta_L=45^\circ$ ). As the regenerator has a filling factor smaller than one ( $f=0.22$ ), and a resistance, it was expected that the best performing orifice diameter would be larger than the calculated optimum.

The phase angle  $\theta_L$  between the pressure and the volume flow, see for example equation (2.21), can be calculated from the measurements.  $\theta_L$  decreases if the orifice diameter increases, and increases if the frequency increases. The phase angle decreases from  $52^\circ$  to  $35^\circ$  if the orifice diameter increases from 0.3 mm to 0.4 mm, with  $f=40$  Hz. With  $f=35$  Hz and an orifice diameter of 0.35 mm  $\theta_L=44^\circ$ , while with  $f=45$  Hz  $\theta_L$  has increased to  $47^\circ$ .

The 0.4 mm orifice diameter has a phase angle  $\theta_L=37^\circ$  with  $f=45$  Hz. This is a smaller phase angle than with the 0.35 mm orifice. Although with the 0.35 mm orifice the phase angle is closer to  $45^\circ$ , the reached  $T_L$  is higher. The optimum for a single orifice pulse tube is both in the experiments and in theory smaller than  $45^\circ$ .

The obtainable cooling power is proportional (in the ideal case equal) to the amount of energy dissipated in the orifice. The dissipation is proportional to the volume flow through the orifice and the pressure amplitude in the tube (equation (2.21) and figure 2.5). The volume flow through the orifice increases if a larger orifice diameter is used, but the pressure amplitude in the tube decreases if  $|\hat{\phi}_H|$  increases. As  $|\hat{p}_t|$  decreases, the pressure difference over the regenerator increases, increasing the volume flow through the regenerator. The volume flow  $|\hat{\phi}_L|$  increases, this results in a pressure amplitude in the tube that decreases a bit less. This results in an increasing cooling power per kelvin if the orifice is enlarged from  $d=0.3$  mm to  $d=0.4$  mm, but the increase is not linear with the orifice resistance.

The pulse tube performs best if an orifice diameter of 0.35 mm is used and the frequency is 35 Hz. The phase angle is 45° and the lowest temperature is reached. However, the cooling power per kelvin is not the highest. According to equation (2.27), the optimal orifice results in the optimal enthalpy flow. This does not mean that the enthalpy flow is maximal, but that the part of the enthalpy flow that results in cooling power is maximal. As the regenerator is not ideal, there will be an enthalpy flow,  $\langle \dot{H}_r \rangle$ , through the regenerator, but  $\langle \dot{H}_r \rangle / \langle \dot{H} \rangle$  is smallest with the 0.35 mm orifice diameter and  $f=35$  Hz. There is an enthalpy flow through the regenerator as the heat transfer between regenerator and gas is finite and the heat capacity of the regenerator is finite. When the gas moves to the cold end the gas inside the regenerator is compressed. The temperature of the gas rises and as the heat transfer is finite, the gas temperature at a certain cross-section is higher than the local regenerator temperature. As the heat capacity of the regenerator is finite, the temperature of the regenerator at a cross-section increases during the compression phase and decreases during the expansion phase. It can be shown that this results in the following expression for the first order change of the oscillating gas temperature  $\hat{T}_g$ , and regenerator temperature  $\hat{T}_r$  [11]

$$\rho_0(1-f)c_p\hat{T}_g + C_0\hat{T}_r = \frac{ic_p\dot{m}}{\omega A_r} \frac{dT_0}{dx} + (1-f)\hat{p}, \quad (4.3)$$

where  $C_0$  is the heat capacity per unit regenerator volume and  $dT_0/dx$  the temperature gradient in the regenerator. For a fixed  $T_L$  the temperature gradient in the regenerator is constant. The expression shows that the amplitude of the gas and regenerator temperature is dependent on the mass flow,  $\dot{m}$ , through the regenerator and the pressure amplitude in the regenerator. If the orifice diameter increases the mass flow through the regenerator increases faster than the pressure amplitude in the regenerator decreases. This results in an increasing enthalpy flow through the regenerator if the orifice diameter increases.

### Measurements

The diamonds in figure 4.5 depict the total enthalpy flow versus the cold heat exchanger temperature. The enthalpy flow is calculated from the measurements with equation (2.58), for a tube with an adiabatic core and a thermal boundary layer. The enthalpy flow is calculated at the low temperature side of the tube. At the warm side of the tube the enthalpy flow is always higher (around ten percent) than at the cold side. The reason for this will be explained a bit further.

The data of the 0.35 mm orifice at a frequency of 35 Hz are given. The enthalpy flow increases from 1.8 to 2.7 W if  $T_L$  rises from 110 to 160 K. The enthalpy flow grows approximately 19 mW/K. This is only half of the cooling power per kelvin (figure 4.4). The squares in figure 4.5 are the calculated normalised losses: the enthalpy flow minus the cooling power (figure 4.3) divided by the enthalpy flow. The normalised losses decrease if the low temperature rises. At the minimum  $T_L$  the normalised losses are equal to one as all the enthalpy flow through the tube is necessary to maintain that temperature. With a cold heat exchanger temperature of 160 K the losses are reduced to only 28 % of the available enthalpy flow.

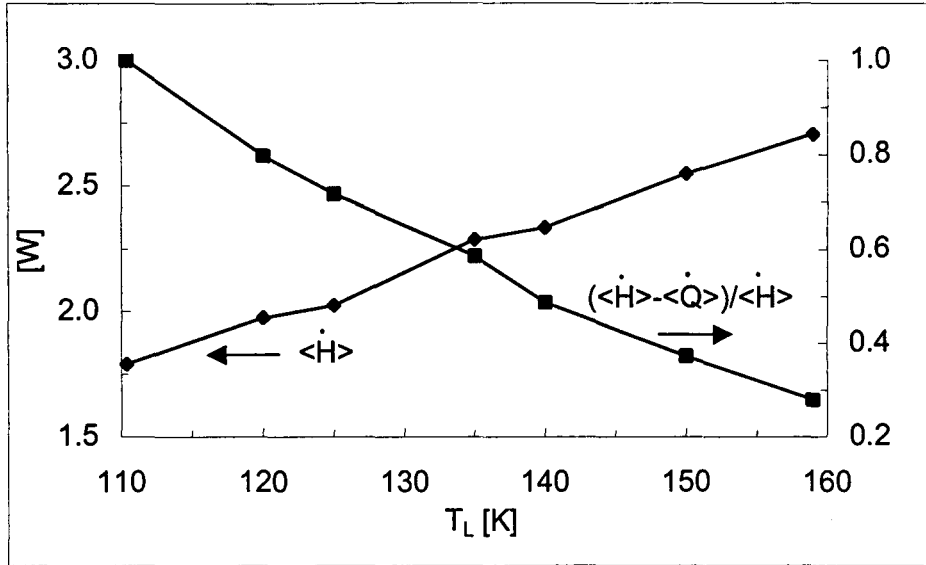


figure 4.5: The enthalpy flow versus cold heat exchanger temperature and normalised cooling power losses versus cold heat exchanger temperature. All calculations are done for the measurements with an orifice diameter of 0.35 mm at a frequency of 35 Hz.

In figure 4.6 the enthalpy flow of figure 4.5 is divided into its three constituents. The total enthalpy flow is the sum of the adiabatic enthalpy flow,  $\langle \dot{H}_{ad} \rangle$ , surface heat pumping,  $\langle \dot{H}_{su} \rangle$ , and the gradient effect,  $\langle \dot{H}_{gr} \rangle$  (see equation (2.59)). All three components increase if  $T_L$  increases. The adiabatic enthalpy flow dominates the total enthalpy flow. The magnitude of the surface heat pumping is very small,  $\langle \dot{H}_{su} \rangle = 0.1$  W if  $T_L = 110$  K and 0.2 W if  $T_L = 160$  K. The gradient effect increases (becomes less negative) from  $-0.8$  W to  $-0.7$  W if  $T_L$  increases. The gradient effect is always more negative than the surface heat pumping component is positive.

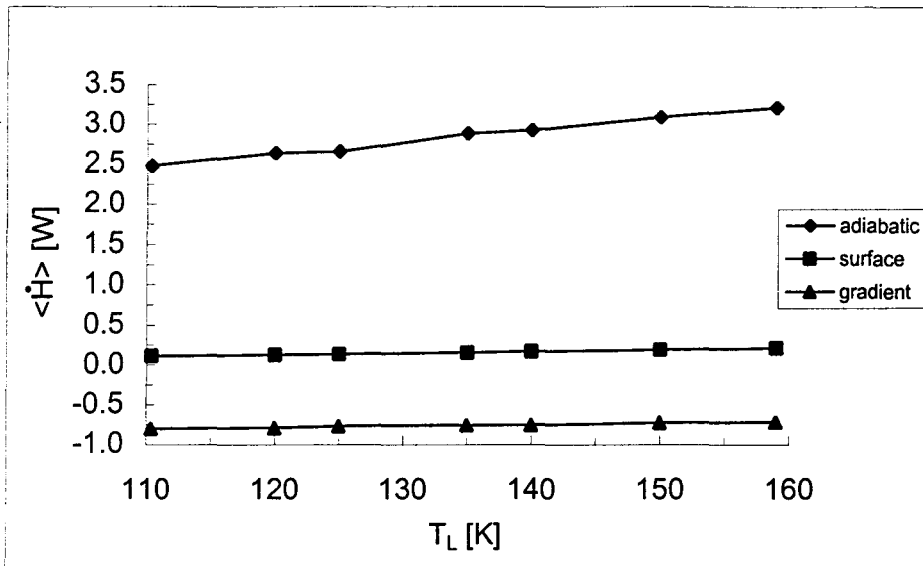


figure 4.6: The total enthalpy flow of figure 4.5 divided into an adiabatic enthalpy flow, surface heat pumping and gradient effect versus the cold heat exchanger temperature.

### Discussion

The enthalpy flow decreases as  $T_L$  decreases, because both the pressure amplitude in the tube and the volume flow entering the tube at the cold side decrease. Gas at the warm end of the regenerator has a lower density than the gas at the cold end of the regenerator. The more the low temperature drops the more the density increases and the more the volume flow decreases. As the pressure build-up is caused by the volume flow entering the tube, a smaller volume flow entering results in a lower pressure amplitude in the tube. Lower pressure oscillations result in a smaller volume flow leaving at the warm side.

The enthalpy flow is higher than the cooling power as there are losses created by an enthalpy flow and heat conduction through the regenerator and heat conduction through the tube's wall. The normalised losses increase as  $T_L$  drops. With a decreasing  $T_L$ , the temperature gradient in both the tube and the regenerator increases. As, according to equation (4.3), the temperature oscillations are proportional to the temperature gradient in the regenerator, the enthalpy flow through the regenerator increases. In the tube, the gradient effect is proportional to the temperature gradient in the tube's wall. However, as this is only in a small boundary layer near the wall the gradient effect is small, whereas in the regenerator all the gas is in thermal contact with the regenerator. The heat conduction through the regenerator and tube's wall increase as  $T_L$  decreases. The heat conduction through the regenerator will increase more than through the tube's wall as there is next to the wall also conduction through the gauzes.

The adiabatic enthalpy flow is much larger than the surface heat pumping and gradient effect as the thermal boundary layer,  $\delta_T$ , is small compared to the tube's radius ( $\delta_T/R_t \approx 0.05$ ). All three components of the enthalpy flow increase if  $T_L$  rises as both the pressure amplitude and the amplitude of the volume flow increase. Although the gradient effect is proportional to the square of the volume flow, it becomes less negative with an increasing  $T_L$ . The reason for this is that the temperature gradient in the wall decreases faster than the volume flow entering the tube increases. If  $|\hat{\phi}_L|$  would

increase linear with the temperature, a temperature increase from 100 K to 150 K increases  $|\hat{\phi}_L|$  with a factor  $150/100=1.5$ , while the temperature gradient,  $\nabla T_0$ , only decreases with a factor  $(300-150)/(300-100)=3/4$ . This would result in a more negative gradient effect. In the experiments, the measured volume flow increases only 10 %, because both the regenerator's flow resistance and the pressure amplitude in the tube increase if  $T_L$  rises. The flow resistance of the regenerator is proportional to the viscosity of helium, and as the viscosity increases if its temperature increases, also  $R_r$  increases [6]

$$R_r = \frac{Z_r'}{L_r} \mu_H \int_0^{L_r} \left(\frac{T}{T_H}\right)^{0.63} \frac{T}{T_L} dx, \quad (4.4)$$

with  $Z_r'$  the flow impedance of the regenerator per unit volume and  $\mu_H$  the viscosity at  $T_H$ . If the temperature gradient over the regenerator is constant, we can integrate the expression. With  $T_H=300$  K and  $T_L=100$  K this results in  $R_r=0.13Z_r'\mu_H$  and if  $T_L=150$  K,  $R_r=0.15Z_r'\mu_H$ .

In equation (2.56), an expression is given for the critical temperature gradient. The critical temperature gradient increases if  $T_L$  rises, but the measured temperature gradient was in all experiments larger. The measured temperature gradient can be up to six times the critical temperature gradient for large volume flows ( $d=0.4$  mm) and low  $T_L$ . However, even with the smallest orifice ( $d=0.3$  mm) and  $T_L=160$  K the measured temperature gradient was still two times larger than the critical temperature gradient. As the gas is compressed, the temperature of the gas is lower than the tube's local wall temperature. This results in a negative gradient effect that is larger than the positive surface heat pumping component. If the cooler is designed in such a way that the phase angle  $\theta$  is small the surface heat pumping component decreases, but the adiabatic enthalpy flow increases, while the gradient effect is unaffected (equation (2.59)). The adiabatic enthalpy flow will increase much more than the surface heat pumping component decreases. In the experiments discussed above, the thermal boundary layer was much smaller than the tube's radius ( $\delta_T/R_t \approx 0.05$ ). This means that surface heat pumping (and the gradient effect) only occurs in 10 % of the tube's cross-section, while the adiabatic enthalpy flow occurs in the other 90 %.

The tube has an adiabatic core with a thermal boundary layer  $\delta_T$ . The size of the boundary layer is dependent on the position in the tube. At the cold side it is approximately five percent of the tube's radius and at the warm side around ten percent. A larger boundary layer together with a smaller volume flow still results in a larger enthalpy flow at the warm side. The adiabatic enthalpy flow is slightly smaller at the warm side of the tube as the volume flow in-phase with the pressure amplitude is constant over the tube's length. Surface heat pumping is also smaller as the volume flow out-of-phase is smaller. The calculated enthalpy flow still increases because of the larger gradient effect (less negative) at the warm side as the volume flow at the warm side is smaller than the volume flow at the cold side.

The real enthalpy flow is constant throughout the tube. The real temperature profile of the gas in the tube is not linear [15]. The temperature gradient is steeper at the warm side than at the cold side. At the cold side the (calculated) enthalpy flow increases as the gradient effect becomes less negative and at the warm side the enthalpy flow decreases as the gradient effect becomes more negative.

## 4.2 The inertance pulse tube

### Measurements

Experiments are done with three inertance diameters. The inertances had a diameter of 0.79 mm, 0.91 mm and 1.32 mm. Each inertance is varied in length. In figure 4.7 the minimum  $T_L$  versus the length is depicted. The figure shows that with the right diameter/length combination the use of an inertance is beneficial. Compared to the orifice pulse tube, the minimum temperature can drop with ten degrees, to a  $T_{L,\min}=100$  K. This temperature is reached with the same mean pressure, frequency and mechanical input power as in the orifice pulse tube cooler. With both an inertance diameter of 0.79 mm and 0.91 mm approximately the same minimum temperature can be reached. If an inertance diameter of 1.32 mm is used, the lowest temperature reached is 122 K.

The shape of the curves is somewhat influenced by the number of points measured. The inertance with a diameter of 0.91 mm is examined the most extensively. The length of this capillary is each time decreased with ten centimetres, while the other two capillaries have larger gaps. The optimum length decreases if the inertance diameter decreases and the optimum becomes more sharp edged. The optimal length is around 2.6 m to 3.1 m if  $d=1.32$  mm, around 1.4 m to 1.6 m if  $d=0.91$  mm and around 0.5 m if  $d=0.79$  mm.

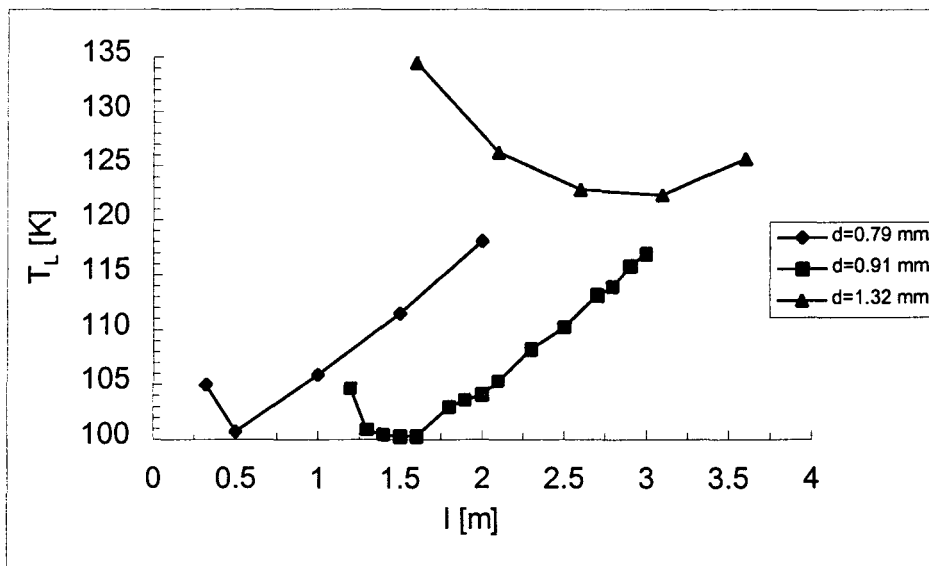


figure 4.7: Minimum cold heat exchanger temperature versus inertance length for three inertance diameters. The mean pressure was 1.6 MPa, the frequency 35 Hz and the mechanical input power 20 W.

### Discussion

The curve of the smallest diameter inertance has a sharp edged minimum. This can be partly due to the fewer measured points. More likely, the curve would also be sharp edged as more points were measured. The resistance of the inertance is, according to equation (2.29), proportional to  $l/d^4$ . The  $d=0.79$  mm inertance has an optimum length of approximately 0.5 m. If the length is increased with ten centimetres,  $l/d^4$  increases from 1.3 m/mm<sup>4</sup> to 1.5 m/mm<sup>4</sup>.  $l/d^4$  increases from 2.2 m/mm<sup>4</sup> to 2.3 m/mm<sup>4</sup> if the optimum length (1.5 m) for the  $d=0.91$  mm inertance is increased with ten centimetres. A smaller diameter results in a larger resistance per unit length. This gives the smallest



inertance diameter the smallest range in length where the resistance/inductance combination is good.

The amount of gas entering the inertance is (for  $d=0.79$  mm and  $d=0.91$  mm) at the optimum length around 20 % of the tube's volume. The amount of gas entering the largest diameter inertance is around 30 % of the tube's volume. The cross-section of the inertance with a diameter of 1.32 mm is too large for this pulse tube. The amount of gas entering and leaving the tube each cycle is that large that the displacement and the velocity of the gas is relative large. The assumption that there is no length-wise mixing in the tube is probably not valid anymore. The volume of the 1.32 mm diameter inertance is at its optimum length  $3.5\text{ cm}^3$ , more than two times larger than the tube's volume. The accumulation of gas in this inertance is large. The capacity of the inertance cancels out the inductance of the inertance.

The pulse tube has no heat exchanger at the warm side of the tube as the construction costs of a heat exchanger are high. For the optimisation of the pulse tube a heat exchanger is not necessary, a pulse tube without a heat exchanger gives the system simplicity. The only difference is that the temperature profile in the tube is steeper than with a heat exchanger. Without a heat exchanger the warm gas leaving the tube mixes with the gas in the buffer. The gas leaving the buffer volume has a lower temperature than the gas entering. This is the case for the orifice pulse tube. In the inertance pulse tube there is an extra volume that separates the tube from the buffer: the volume of the inertance. Not all the gas leaving the tube will mix with the gas in the buffer. As the inertance diameter increases the optimum length increases and also the volume of the inertance. If the smallest inertance diameter is used the volume of the amount of gas leaving the tube is larger than the inertance volume. Around one third of the warm gas leaving the tube will mix with the gas in the buffer. The other two inertances have each a volume that is larger than the warm gas's volume. None of the gas leaving the tube will mix with the gas in the buffer. The temperature of the gas returning to the tube will still have a lower temperature than when it left. Heat transfer from the gas to the inertance wall will lower the gas's temperature.

## Measurements

More experiments are done with the 0.91 mm diameter inertance. The mean pressure and the frequency are varied. For each frequency/mean pressure combination, the optimum inertance length is determined. The results of these experiments are given in table 4.1. The minimum  $T_L$ , the cooling power per kelvin and the enthalpy flow at the cold side of the tube for  $T_{L,\min}$  are also given.

The table shows that the differences between the different combinations are quite small. The maximal difference in  $T_{L,\min}$  is 4 K and the maximal difference in optimum length forty centimetres. There are a few trends to see. A higher frequency results in a smaller optimum length. A higher mean pressure results in a larger optimum length. A larger inertance diameter results in a larger optimum length as can be seen in figure 4.7. Finally, a higher mean pressure results in a higher cooling power per kelvin. For a constant mean pressure, the highest cooling power per kelvin is obtained with a frequency of 40 Hz.

table 4.1: Overview of the measurements with an inertance diameter of 0.91 mm. The mechanical input power was 20 W.

$f$ [Hz]	$p_0$ [MPa]	$l_{opt}$ [m]	$T_{L,min}$ [K]	$\Delta\langle\dot{Q}\rangle/\Delta T_L$ [mW/K]	$\langle\dot{H}\rangle$ [W]
30	1.2	1.5	104	38	1.5
	1.6	1.6	103	42	1.9
	2.0	1.7	103	46	2.1
35	1.2	1.5	100	40	1.6
	1.6	1.5	100	46	1.9
	2.0	1.6	101	48	2.2
40	1.2	1.3	101	41	1.6
	1.6	1.3	100	46	2.1
	2.0	1.3	101	50	2.2
45	1.2	1.3	103	39	1.7
	1.6	1.3	102	45	2.1
	2.0	1.3	103	48	2.4

With a length of 1.4 m, a frequency of 35 Hz and a mean pressure of 2.0 MPa, the mechanical input power is varied. Lower temperatures can be reached if the mechanical input power increases, see the diamonds in figure 4.8. If the input power is increased, both the pressure amplitude and the volume flow increase, but  $\hat{p}_i$  increases faster. The lowest temperature measured is 97 K with an input power of 30 W. The cooling power per kelvin increases as the input power is increased. The highest cooling power per kelvin measured is 65 mW/K with an input power of 30 W. If the input power is 10 W there is 3.5 mW/K per input watt, while with 30 W it is decreased to 2.2 mW/K per input watt. At a temperature  $T_L=120$  K the coefficient of performance  $\xi=0.02$  with an input power of 10 W and  $\xi=0.05$  with an input power of 30 W. For  $T_L=142$  K or higher the  $\xi$  with an input power of 10 W is higher than with 30 W input power.

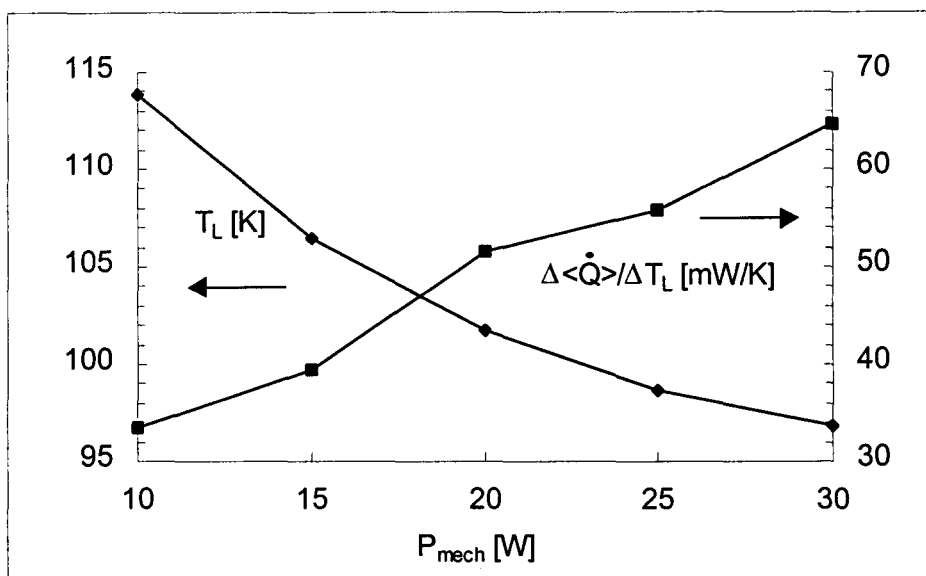


figure 4.8: Minimum cold heat exchanger temperature and the cooling power per kelvin versus mechanical input power. The inertance diameter was 0.91 mm and the length 1.4 m. The mean pressure was 2.0 MPa and the frequency 35 Hz.

## Discussion

In section 2.4.2 it was deduced that the optimal resistance of the inertance is proportional to the tube's capacity and the inertance's inductance

$$\begin{aligned}
 R_{\text{opt}} &= \frac{1}{\omega C_t} - \omega L \\
 &= \frac{\gamma p_0}{\omega V_t} - \omega \frac{4\rho_0 l}{\pi d^2},
 \end{aligned}
 \tag{4.5}$$

and that the resistance is proportional  $l/d^4$ . The trends can be qualitative explained with this equation. Each time the optimal situation is assumed and one parameter is varied while all other variables are kept constant.

With a higher frequency, the optimal resistance decreases. The first term on the right side of equation (4.5) decreases and the second term increases, resulting in a smaller difference. The length interval where approximately the same low temperatures can be reached becomes shorter. If the frequency is 35 Hz the length interval is around thirty centimetres and with a frequency of 45 Hz it shrunk to around ten centimetres. A higher mean pressure increases the optimal resistance. Both terms on the right side of the equation are linear proportional to the mean pressure. The difference increases linear with the mean pressure and thus also the inertance length. A larger inertance diameter leaves the first term unaffected, while the second term decreases, resulting in a larger difference, and as the resistance per unit length decreases, this results in a larger optimum length.

This explains the results only qualitatively. According to the data in table 4.1, increasing the pressure with one third results in an increase in length with less than ten percent. In this discussion the flow in the inertance was assumed laminar while in reality it is oscillating and probably turbulent. The peak Reynolds's number is in the inertance always larger than 2300, and the phenomena at the entrance of the inertance are neglected.

In the last column of table 4.1 the enthalpy flow at the minimum low temperature is given. The phase angle  $\theta_L \approx 30^\circ$ , at the optimum inertance length. This is smaller than in the orifice pulse tube, resulting in a larger enthalpy flow in the inertance pulse tube with the same  $p_0$  and input power.

The enthalpy flow grows if the mean pressure increases resulting in a higher cooling power per kelvin. This enthalpy flow at  $T_{L,\text{min}}$  is proportional to the amount of enthalpy flowing through the regenerator to the cold heat exchanger, as the heat conduction is approximately constant. The heat conduction  $\langle \dot{Q} \rangle$  through the tube's wall is given by [12]

$$\langle \dot{Q} \rangle = -2\pi R_t d_w \lambda_w \frac{dT}{dx},
 \tag{4.6}$$

with  $d_w$  the wall thickness and  $\lambda_w$  the heat conduction coefficient of the wall. The minimum cold heat exchanger temperature is approximately independent of the mean pressure, resulting in a constant temperature gradient in the tube's wall. With  $T_L=100$  K and  $T_H=300$  K, the sum of the heat conduction through the regenerator and tube wall is approximately 0.4 W. With a higher mean pressure  $\langle \dot{H} \rangle$  grows, but  $\langle \dot{H}_t \rangle$  grows just as hard.

For small volume changes, equation (4.2) can be written as

$$p \cong p_0 - \hat{p} \cos \omega t = \frac{mR_m T}{V_0^\alpha} \left(1 - \frac{\hat{V}}{\alpha V_0} \cos \omega t\right). \quad (4.7)$$

If the mean pressure is increased, the pressure amplitude increases and the volume flow decreases. The pressure amplitude increases, as both the mean pressure and the pressure amplitude are proportional to  $mR_m T/V_0^\alpha$ . The volume flow decreases, as the magnitude of the volume flow is proportional to the piston stroke of the compressor. When a constant amount of power is applied to the compressor  $\langle \dot{W} \rangle = \langle p dV \rangle$ , a higher pressure amplitude must result in a smaller piston stroke. The pressure amplitude  $|\hat{p}|$  increases, but the ratio of pressure amplitude and mean pressure,  $|\hat{p}|/p_0$ , decreases. As the input power is constant, this means that the mass flow  $\dot{m} \propto p_0 |\hat{V}|$  must increase. The mass flow increases faster than the pressure amplitude.

The function of the regenerator is to impose locally isothermal conditions on the gas. The regenerator absorbs heat from each particle flowing to the cold side. If the mass flow increases more particles pass a cross-section, the regenerator has to absorb and store more energy. Apparently, the heat capacity  $C_0$  of the regenerator is too small. If we look at equation (4.3),  $C_0$  should be that large that an increase in pressure amplitude and mass flow increases the temperature amplitude of the regenerator and gas only slightly. The temperature oscillations in the regenerator are then much smaller than in the tube, resulting in a smaller increase in  $\langle \dot{H}_r \rangle$ . During the experiments, the outside surface of the warm end of the regenerator becomes warmer than the rest of the cooler. This makes the temperature gradient in the regenerator larger than the temperature gradient in the tube, increasing the temperature oscillations in the regenerator.

If the mean pressure increases the mass flow passing a cross-section of the regenerator grows relative more than the enthalpy flow. If the mechanical input power is increased the enthalpy flow grows relative more than the mass flow passing a cross-section of the regenerator. When the input power is increased, the piston stroke increases, increasing  $|\hat{V}|$ . In this situation the pressure amplitude increases faster than the mass flow. When the input power is increased, lower temperatures can be reached. The enthalpy flow through the tube  $\langle \dot{H} \rangle$  increases more than the enthalpy flow through the regenerator  $\langle \dot{H}_r \rangle$ . Apparently, the influence of the mass flow on the temperature oscillations in the regenerator is larger than the influence of the pressure oscillation.

### 4.3 The double inlet pulse tube

#### Measurements

Some experiments are done with a double inlet pulse tube. For this, an inertance pulse tube is tested with three different bypass orifices. The inertance had a diameter of 0.91 mm and its length was 1.2 m. The used bypass orifices had a diameter of 0.1, 0.3 and 0.4 mm. The lowest temperature reached with a bypass orifice of 0.4 mm was 142 K and is therefore not depicted in figure 4.9. The minimum low temperatures obtained

with the other two bypass orifices together with the data of the inertance pulse tube are depicted in figure 4.9.

With a bypass orifice lower temperatures can be reached than with a “normal” inertance pulse tube. The lowest temperature measured is 96 K with a bypass orifice diameter of 0.3 mm, a mean pressure of 1.2 MPa, a frequency of 40 Hz and an input power of 20 W. This is 6 K lower than without the bypass orifice. With a mean pressure of 1.6 MPa or 2.0 MPa, a bypass orifice diameter of 0.3 mm results also in the lowest temperatures. The pressure amplitude in the tube is 5 % higher when  $d_2=0.3$  mm is used than in the inertance pulse tube. The phase angle  $\theta_L$  could not be determined as the phase of the volume flow  $\hat{\phi}_2$  could not be determined.

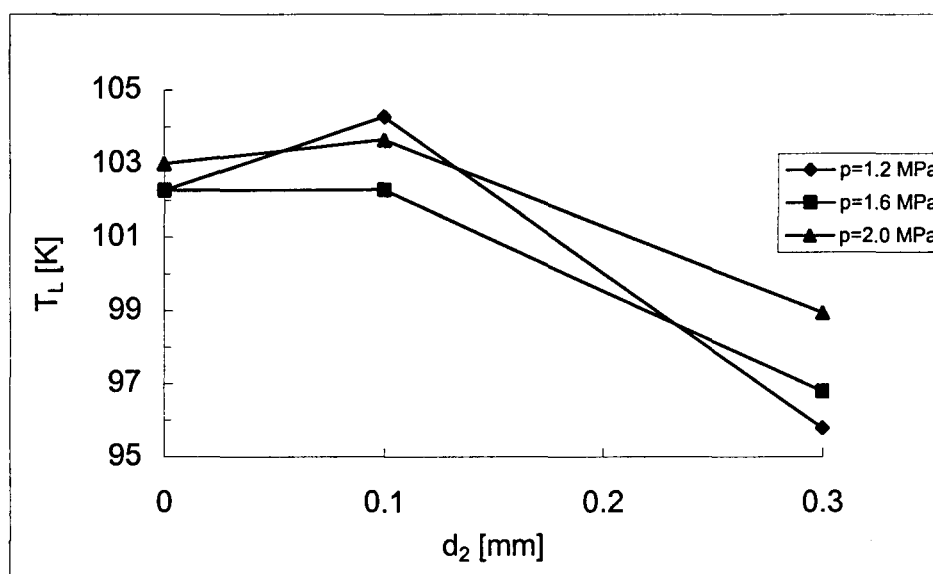


figure 4.9: Minimum cold heat exchanger temperature versus bypass orifice diameter. The inertance had a diameter of 0.91 mm and a length of 1.2 m. The frequency was 40 Hz and the mechanical input power 20 W.

### Discussion

It is assumed that we can calculate the optimal bypass orifice  $R_2$  with equation (2.49). From the experiments, the regenerator's resistance is estimated with the volume flow entering the tube at the low temperature side. For  $T_L=100$  K,  $R_r=3.5 \cdot 10^8$  Pa·s·m<sup>-3</sup>. This results in  $R_{2,opt}=0.2$  GPa·s·m<sup>-3</sup>. This is six times smaller than the resistance of the used best performing orifice. The 0.3 mm diameter orifice has  $R=1.2$  GPa·s·m<sup>-3</sup>, indicating that we underestimate the regenerator's resistance. If the regenerator's capacity is neglected in equation (2.49) the bypass resistance increases to  $R_{2,opt}=0.4$  GPa·s·m<sup>-3</sup>, still much smaller than the resistance of the best performing bypass orifice. The regenerator's resistance cannot be estimated from the measurements.

The pressure amplitude in the tube increases if a bypass orifice is used. The sum of the dissipation in the regenerator and bypass orifice is smaller than the dissipation in the regenerator in an inertance pulse tube.

# Chapter 5

## The 70 mm pulse tube cooler

In this chapter the experiments of the pulse tube cooler with both the pulse tube and regenerator 70 mm long will be discussed. The structure is the same as in chapter 4. In the first section the experiments with the orifice pulse tube cooler will be discussed. One orifice diameter has been tested at various mean pressures and frequencies. The influence of the size of the buffer has been examined with two orifice diameters. In section 5.2 the experiments with the inertance pulse tube will be discussed. The length of one inertance has been varied. At the optimum length/diameter combination the mechanical input power has been increased. In the last section, the double inlet pulse tube will be examined. The orifice diameter of the bypass has been varied and with the best performing bypass orifice the mechanical input power has been increased.

### 5.1 The orifice pulse tube

The volume of this tube is larger than in the 55 mm pulse tube. The diameter of both tubes is the same but the length is increased:  $V_{t,70} = \frac{70}{55} V_{t,55}$ . With equation (2.26) the optimal resistance for this pulse tube can be calculated, as the capacity is linear with the volume:

$$R_{\text{opt},70} = \frac{1}{\omega C_{t,70}} = \frac{55}{70} R_{\text{opt},55}. \quad (5.1)$$

In the 55 mm pulse tube, the best performance was reached with an orifice diameter of 0.35 mm. The resistance of this orifice is  $1.0 \text{ GPa}\cdot\text{s}\cdot\text{m}^{-3}$ , which results in an optimal resistance of  $0.8 \text{ GPa}\cdot\text{s}\cdot\text{m}^{-3}$  for the 70 mm pulse tube. In section 3.3, it is deduced that the resistance is proportional to  $d^3$ , which gives an optimal orifice diameter of 0.38 mm for this pulse tube.

If equations (2.26) and (3.7) are used together with the assumption that the oscillating flow resistance is three times smaller than the DC flow resistance, this results in an optimal orifice diameter of 0.46 mm for  $f=40$  Hz. In section 4.1 the optimal orifice diameter was calculated in this manner, but the experiments showed that the orifice diameter was estimated to large.

#### Measurements

The first experiments are done with an orifice diameter of 0.4 mm. The mean pressure and frequency are varied. The results of these experiments are depicted in figure 5.1. If the mean pressure is increased, lower temperatures can be reached, but the shape of the frequency-temperature curve is the same. The reachable  $T_L$  lowers if the frequency is increased from 35 Hz to 40 Hz.  $T_L$  stays the same as the frequency is further increased to 45 Hz, and increases again when the frequency is increased to 48 Hz. The lowest temperature measured is 101 K at a frequency of 40 and 45 Hz and a mean pressure of 2.0 MPa. The figure shows that lower temperatures can be reached if the mean pressure is increased. The low temperature drop is around 8 K if the mean pressure is increased

from 1.2 to 1.6 MPa and around 4 K when the pressure is increased from 1.6 to 2.0 MPa. Although the temperature drop becomes smaller, it is still substantial.

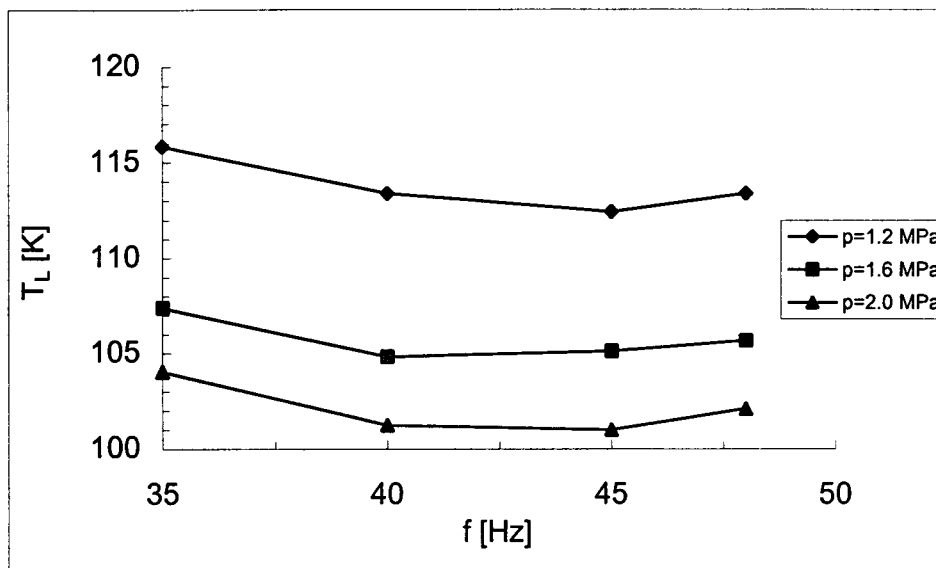


figure 5.1: Cold heat exchanger temperature versus frequency at three mean pressures. The orifice diameter was 0.4 mm and the mechanical input power 20 W.

The squares in figure 5.2 depict the cooling power as a function of  $T_L$ . The figure shows the results of the measurements with the 0.4 mm orifice diameter, at a frequency of 40 Hz and a mean pressure of 1.6 MPa. The cooling power increases as the low temperature is raised. The cooling power per kelvin is 23 mW/K. In the same figure, the triangles depict the enthalpy flow at the cold side of the tube (calculated with equation (2.58)). With an increasing low temperature, the enthalpy flow increases. The enthalpy flow increases approximately 15 mW/K. The enthalpy flow at a certain  $T_L$  is higher than the cooling power at the same low temperature. The difference between the two is equal to the losses in the system. The normalised losses (the diamonds in figure 5.2) decrease as  $T_L$  increases, as the cooling power increases faster than the enthalpy flow.

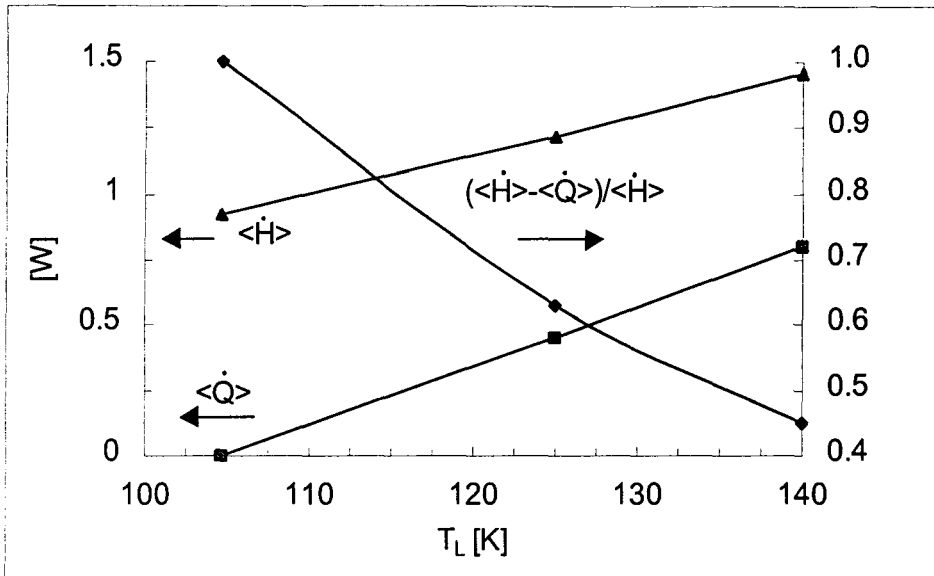


figure 5.2: The cooling power, enthalpy flow and normalised cooling power losses versus cold heat exchanger temperature. The orifice diameter was 0.4 mm, the frequency 40 Hz, the mean pressure 1.6 MPa and the mechanical input power 20 W.

## Discussion

Comparison of these results with the 55 mm pulse tube cooler (figure 4.2) indicates that this cooler's performance is better than the 55 mm pulse tube cooler. The minimum low temperature reached with the 55 mm pulse tube was 110 K (with a mean pressure of 1.6 MPa and a mechanical input power of 20 W). With the 70 mm pulse tube a low temperature of 105 K is reached (with the same mean pressure and mechanical power input). A higher filling factor ( $f=0.29$  in this cooler and 0.22 in the 55 mm cooler) and a longer regenerator make it possible to reach lower cold heat exchanger temperatures.

The cooling power per kelvin is with this cooler only half of the 55 mm cooler (see figure 4.4). The reason for this is that the enthalpy flow through the tube is smaller than in the former cooler (figure 4.5). The enthalpy flow is smaller due to a smaller pressure amplitude and amplitude of the volume flow in the tube if the same mechanical power is applied to the compressor. The regenerator has a higher filling factor, which increases the flow resistance of the regenerator. This results in a larger pressure drop over the regenerator. A second reason why the pressure amplitude in the tube is smaller is the larger volume of both the tube and the regenerator. A part of the volume flow entering the regenerator at the warm side will accumulate in the regenerator. The void volume of the regenerator  $V_{r,70} = \frac{(1-0.29)^{70}}{(1-0.22)^{55}} V_{r,55} = 1.2V_{r,55}$ . As the amount of void volume is larger, the volume flow entering at the cold side of the tube decreases. With a smaller volume flow entering, the gas in a larger tube's volume has to be compressed. The ratio of pressure amplitude and mean pressure in the tube,  $|\hat{p}_t|/p_0$ , decreases. The ratio is half of the ratio in the former cooler,  $|\hat{p}_t|/p_0 \approx 0.05$  to 0.1 in the 55 mm pulse tube.

The losses are mainly created by an enthalpy flow through the regenerator and heat conduction through the wall. The enthalpy flow increases less quickly than the cooling power, but the difference between the two is in this pulse tube smaller than in the 55 mm pulse tube. The losses are reduced to almost 50 % of the losses in the former cooler.



The heat conduction  $\langle \dot{Q} \rangle$  (equation (4.6)) through the wall's is for the same temperature difference smaller, as the length is longer. With  $T_L=100$  K and  $T_H=300$  K, the sum of the heat conduction through the regenerator and tube wall is approximately 0.3 W. If all other losses are assumed to be due to the enthalpy flow through the regenerator,  $\langle \dot{H}_r \rangle = \langle \dot{H} \rangle - \langle \dot{Q} \rangle \approx 0.6$  W, this is smaller than in the 55 mm pulse tube:  $\langle \dot{H}_r \rangle \approx 1.8 - 0.4 = 1.2$  W. This can be understood with equation (4.3). Both terms on the right side of the equation are smaller. The mass flow is smaller as the volume flow is smaller; the temperature gradient  $dT_0/dx$  is smaller, as the regenerator is longer. The filling factor is higher and the pressure amplitude is smaller. On the left side of the equation,  $C_0$  increases with a factor  $0.29/0.22=1.3$ , as the filling factor is higher, because of the same reason the pre-factor for  $\hat{T}_g$  decreases with a factor 0.9. The temperature oscillation of the gas in the regenerator decreases as most is absorbed by the regenerator term. The absolute losses are much smaller than in the 55 mm pulse tube, but relative it is only slightly smaller as also the enthalpy flow is smaller. The normalised losses are approximately 10 % smaller than in the 55 mm cooler (figure 4.5).

### Measurements

Some experiments are done with an orifice diameter of 0.35 mm, at a mean pressure of 2.0 MPa. The results of these experiments together with the 0.4 mm orifice diameter are depicted in figure 5.3. The influence of the size of the buffer volume is examined. The buffer volume is extended (the open symbols in figure 5.3) to a size that is more than three times larger than the normal buffer size. With an extended buffer volume, lower temperatures can be reached than with a "normal" sized buffer. The lowest temperature reached is 91 K with an orifice diameter of 0.35 mm, a frequency of 30 Hz and an extended buffer volume. With a "normal" sized buffer, the lowest temperature reached is 94 K with the same settings.

The phase angles between the pressure amplitudes in buffer and tube increase a few degrees if an extended buffer is used. This results in (calculated) phase angles  $\theta_L$  that decrease a few degrees if an extended buffer is used. The volume flow at the warm end of the tube is approximately the same for a normal and an extended buffer.

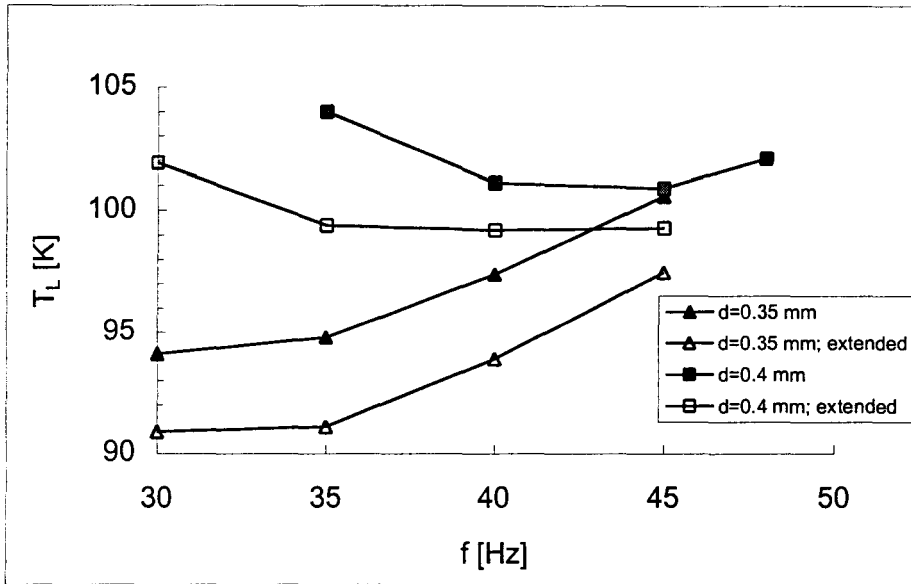


figure 5.3: Cold heat exchanger temperature versus frequency for two orifice diameters. The buffer volume was  $37 \text{ cm}^3$  for the data with the closed symbols and  $122 \text{ cm}^3$  for the data with the open symbols. The mean pressure was  $2.0 \text{ MPa}$  and the mechanical input power  $20 \text{ W}$ .

## Discussion

The reached cold heat exchanger temperatures with an extended buffer are lower, as the mean temperature in the extended buffer is lower. The refrigerator has no heat exchanger at the warm side of the tube. The gas leaving the tube at the warm side mixes with the gas in the relatively large buffer. The gas returning to the tube has approximately the temperature of the gas in the buffer. As warm gas enters the buffer, the temperature of the gas in it increases. This temperature increase is smaller if the buffer is larger. With the extended buffer, the gas returning to the tube has a lower temperature. The temperature of the warm end of the tube is lower, which results in a smaller temperature gradient in the tube's wall if the cold heat exchanger temperature is the same.

The larger phase angle between the pressure amplitude in the buffer and tube is a direct result of the larger capacity. In equation (2.24), the buffer capacity  $C_b$  was neglected as it is relative large. In this situation, the volume flow  $|\hat{\phi}_H|$  will be in-phase with the pressure amplitude in the tube  $|\hat{p}_t|$ . In reality,  $|\hat{\phi}_H|$  is before in phase of  $|\hat{p}_t|$  as the buffer capacity is finite. When the buffer is extended, the phase angle between  $|\hat{\phi}_H|$  and  $|\hat{p}_t|$  becomes smaller (the phase angle decreases from  $11^\circ$  to  $5^\circ$  for  $f=35 \text{ Hz}$  and  $d=0.35 \text{ mm}$ ).

The enthalpy flow is with the extended buffer larger. The adiabatic enthalpy flow becomes larger as the volume flow in-phase with the pressure is larger. Surface heat pumping becomes smaller as the volume flow out-of-phase becomes smaller. The gradient effect is unaffected by a larger buffer volume, as both the warm end temperature and the cold end temperature drop.

The measured phase angle (for a normal buffer size) is around  $40^\circ$  with an orifice diameter of  $0.35 \text{ mm}$  ( $f=40 \text{ Hz}$ ), and  $\theta_L \approx 35^\circ$  with  $d=0.4 \text{ mm}$ . These (calculated from the

measurements) phase angles are somewhat smaller than with the same settings in the 55 mm pulse tube cooler. According to section 2.4.1 the phase angle should be larger than in the 55 mm pulse tube as the capacity of this tube is larger. Nevertheless, the phase angle is smaller due to a smaller resistance. During the experiments with the 70 mm orifice pulse tube cooler the ratio of the pressure amplitudes in buffer and tube was larger than with the same settings in the 55 mm pulse tube cooler. The pressure drop over the orifice was smaller, resulting in a smaller resistance of the orifices. This can be due to e.g. a different placed O-ring or the plate between the orifice and the tube being turned somewhat.

## 5.2 The inertance pulse tube

### Measurements

The experiments with an inertance pulse tube are done with an inertance diameter of 1.02 mm. The inertance length and the mean pressure are varied. The results of these experiments are depicted in figure 5.4. The experiments with an orifice pulse tube showed that the minimum cold heat exchanger temperature drops if the mean pressure is increased (figure 5.1). In the experiments with the inertance pulse tube, the mean pressure is increased even more. The results in figure 5.4 show that it is profitable to increase the mean pressure further. The minimum  $T_L$  drops, although the differences become smaller. The cold heat exchanger temperature difference between a mean pressure of 2.0 MPa and 2.8 MPa is only 3 K. The lowest temperature reached is 84 K with an inertance length of 1.7 m and a mean pressure of 2.8 MPa.

The optimum length increases if the mean pressure is increased. An exception is the optimum length with  $p_0=1.2$  MPa,  $l_{opt}\approx 1.5$  m, while with a mean pressure of 1.6 MPa a shorter optimum length is found ( $l_{opt}\approx 1.4$  m).

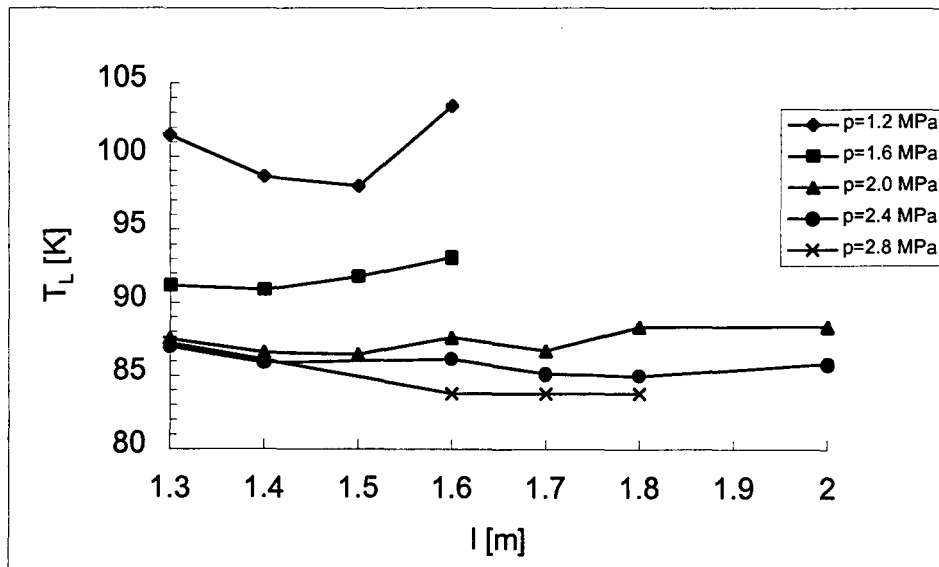


figure 5.4: Minimum cold heat exchanger temperature versus inertance length. The inertance had a diameter of 1.02 mm. The frequency was 35 Hz and the mechanical input power 20 W.

### Discussion

The optimum inertance lengths are approximately the same as found for the 55 mm pulse tube (table 4.1). The inertance has a larger diameter ( $d=1.02$  mm compared to

$d=0.91$  mm), but this pulse tube has also a larger volume. Both the volume of the tube as the cross-section of the inertance have increased the same amount. According to equation (4.5), the optimal resistance will be the same and is the resistance proportional to  $l/d^4$ . Again the experiments show that this formula explains the results only qualitatively. With this formula the optimum length would be larger than found for the 55 mm pulse tube, while it is approximately the same as in the 55 mm pulse tube.

### Measurements

At the optimum length of the inertance, the mechanical input power is increased. The results of these experiments are depicted in figure 5.5. With a mean pressure of 2.4 MPa or 2.8 MPa and a frequency of 35 Hz, the optimum length is 1.7 m. The lowest temperature reached is 78 K, with a mean pressure of 2.8 MPa and a mechanical input power of 35 W.

With a mean pressure of 2.8 MPa lower temperatures can be reached than with the same settings but a mean pressure of 2.4 MPa. At an input power of 20 W the low temperature difference is 1 K. Raising the input power decreases the minimum temperature difference. At an input power of 35 W the low temperatures are almost equal.

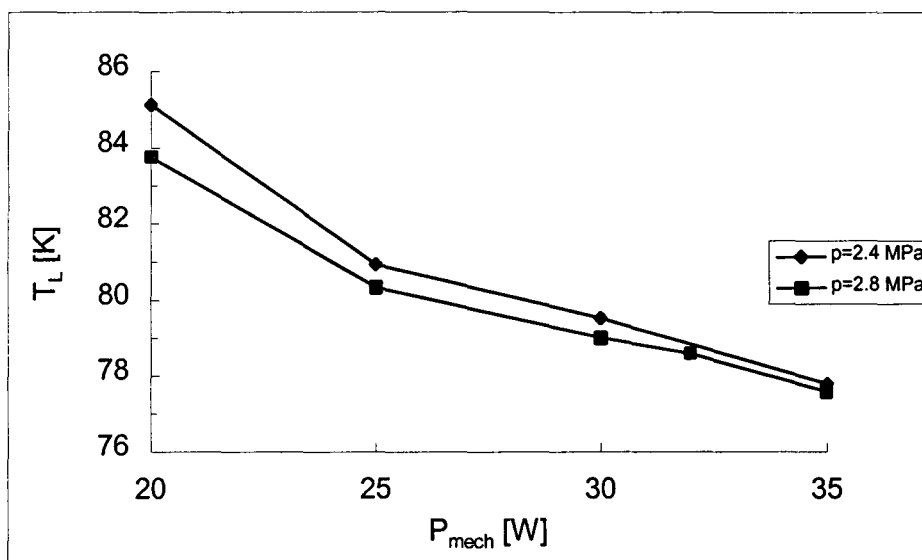


figure 5.5: Cold heat exchanger temperature versus mechanical input power. The inertance had a diameter of 1.02 mm and a length of 1.7 m. The frequency was 35 Hz.

As the mechanical input power is raised, the warm end of the regenerator becomes warmer. The temperature of the warm end is measured with a thermocouple. The thermocouple is stuck at the warm end surface of the regenerator. The gas temperature passing the warm end of the regenerator will be higher. In table 5.1 the surface temperature at different input powers is given. The surface temperature increases with an increasing mechanical input power. With an input power of 20 W the surface temperature is approximately twenty degrees above room temperature. Raising the input power to 35 W increases the surface temperature ten degrees more.

The surface temperature of the warm end of the tube is also measured. The temperature increases as the mechanical input power increases, but not as much as the warm end of

the regenerator does. With an input power of 20 W the surface temperature is 25° C and with an input power of 35 W the temperature is three degrees higher.

*table 5.1: Surface temperature of the warm end of the regenerator at different mechanical input powers. The mean pressure was 2.8 MPa.*

$P_{\text{mech}}$ [W]	$T$ [°C]
20	41
25	43
30	48
35	51

### Discussion

A higher mechanical input power increases the piston stroke of the compressor. Both the volume flow and the pressure amplitude in the tube increase. The enthalpy flow through the tube increases, with as a consequence that the cooling power at a fixed cold heat exchanger temperature increases and the reachable minimum temperature drops. The temperature of the warm side of the regenerator increases with a higher input power. This indicates that a heat exchanger at the warm end is necessary to reject the heat to the surroundings. There is an enthalpy flow through the tube connecting the compressor with the regenerator. Most of this enthalpy flow is blocked at the warm end of the regenerator. Heat is absorbed by the regenerator and as the regenerator does not reject much heat to the surroundings the temperature of the warm end increases. As the temperature of the warm end increases, the temperature gradient in the regenerator increases (for a fixed cold heat exchanger temperature). According to equation (4.3), the temperature oscillations in the regenerator increase, increasing the enthalpy flow through the regenerator. Secondly, the heat conduction through the regenerator also increases. If the warm end temperature would be at room temperature the temperature gradient decreases, decreasing both the enthalpy flow through the regenerator and the heat conduction. Lower cold heat exchanger temperatures should be reachable.

## 5.3 The double inlet pulse tube

### Measurements

Experiments are done with three bypass orifice diameters. The bypass orifice is used in an orifice pulse tube cooler (the diamonds in figure 5.6) and in an inertance pulse tube (the squares in figure 5.6). The best performing orifice and inertance are chosen for a frequency of 35 Hz: an orifice with a diameter of 0.35 mm and an inertance with a diameter of 1.02 mm and 1.7 m in length. The mean pressure was 2.8 MPa and the mechanical input power 20 W. When the orifice is used the normal buffer size is used.

With a bypass orifice diameter of 0.2 mm the lowest temperatures are reached in both the orifice and inertance pulse tube. In the orifice pulse tube a low temperature of 88 K is reached and in the inertance pulse tube a low temperature of 79 K. The bypass orifices  $d_2=0.15$  mm and  $d_2=0.2$  mm are also turned around. The obtained temperatures can differ quite a lot. For the 0.15 mm bypass orifice the difference is 5 K, while with the 0.2 mm bypass orifice the difference is only 0.5 K.

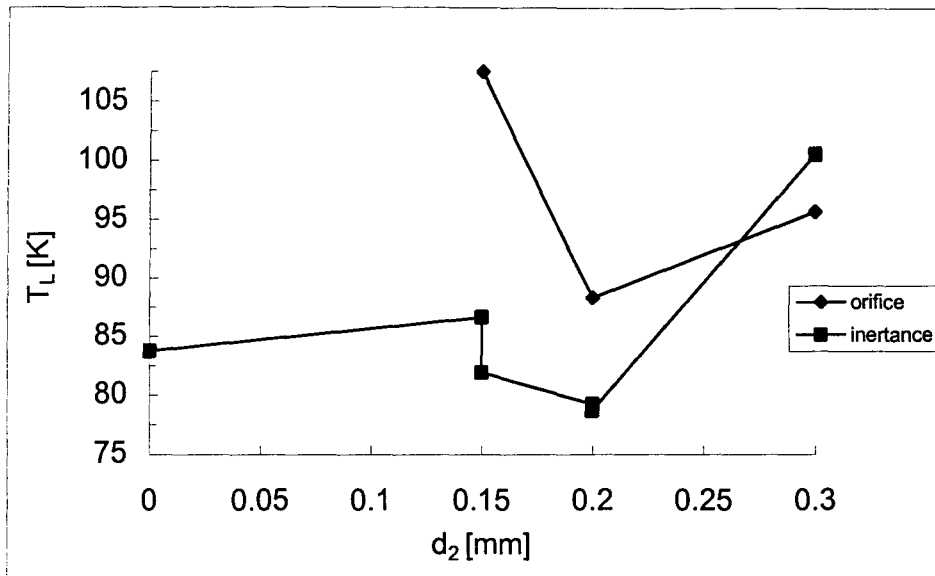


figure 5.6: Minimum cold heat exchanger temperature versus diameter of the bypass orifice. The orifice had a diameter of 0.35 mm and the inertance a diameter of 1.02 mm and a length of 1.7 m. The frequency was 35 Hz, the mean pressure 2.8 MPa and the mechanical input power 20 W.

The mechanical input power is increased with the inertance pulse tube and a bypass orifice of 0.2 mm. The lowest temperature reached is 73 K. This can be reached with an input power of 30 W if the mean pressure is 2.8 MPa, and with an input power of 35 W if the mean pressure is 2.4 MPa.

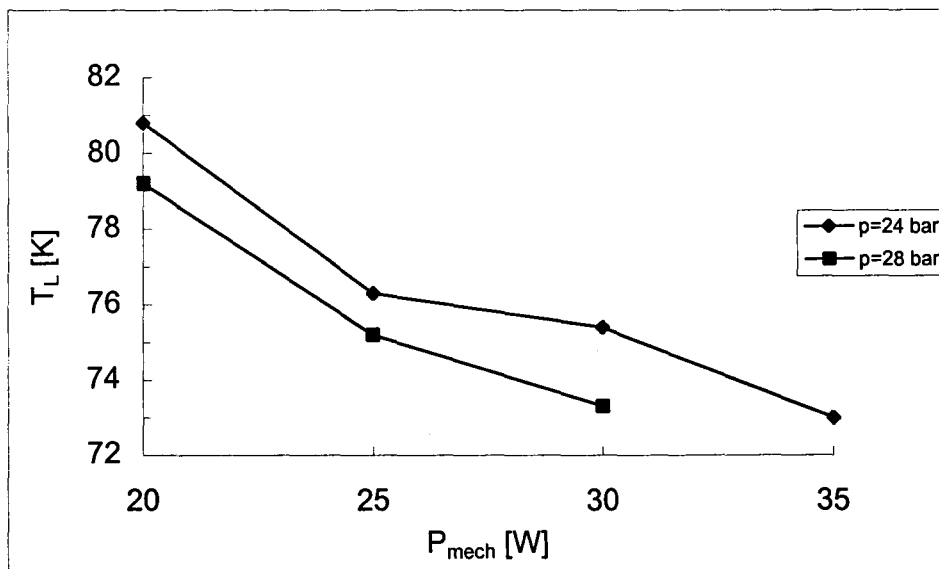


figure 5.7: Cold heat exchanger temperature versus mechanical input power. The inertance had a diameter of 1.02 mm and a length of 1.7 m. The diameter of the bypass orifice was 0.2 mm. The frequency was 35 Hz.

## Discussion

In section 4.3, the size of the optimal bypass orifice was estimated with equation (2.49). This gave very poor results as the resistance of the regenerator could not be determined. In this section the resistance of the regenerator is taken to be  $R_{r,70} \approx 5R_{r,55}$  as the pressure drop over the regenerator is around 50 % and in the 55 mm pulse tube cooler around 10 %. With equation (2.49), this results in a bypass orifice resistance of  $R_2 = 1.7 \text{ GPa}\cdot\text{s}\cdot\text{m}^{-3}$ , or  $d_2 = 0.27 \text{ mm}$ . This is larger than the found best performing orifice diameter of 0.2 mm, but orifices with diameters closer to 0.27 mm are not tested. The best performing bypass orifice has a larger resistance than in the 55 mm pulse tube, as  $R_{r,70} > R_{r,55}$ .

When the bypass orifice is turned around the reachable  $T_L$  can differ. The reason for this is that the orifice is not symmetric. The flow resistance in one direction can differ from the flow resistance in the opposite direction. This was already noticed in the steady flow measurements in section 3.3. A DC gas flow circles through the regenerator, tube via the bypass orifice back to the warm end of the regenerator or in the opposite direction. This flow should not be seen like a real DC flow but rather like an asymmetric flow. With the bypass orifice there is a closed-loop created, with the potential for a DC gas flow. The amount of gas passing a cross-section in one direction during half a cycle, is not the same amount of gas passing in the opposite direction during the next half cycle. The DC flow carries an additional thermal loss and can significantly raise the temperature. If the tube is assumed adiabatic, a DC flow which travels from the warm to the cold side results in a loss given by  $\langle \dot{H}_H \rangle - \langle \dot{H}_L \rangle = \dot{m}_{DC} c_p (T_H - T_L)$ , where  $\dot{m}_{DC}$  is the DC component of the mass flow. The DC flow results from the fact that two non-linear impedances (regenerator + tube and bypass orifice) are parallel. Only if both impedances follow an identical pressure drop versus mass flow no DC flow would appear. In practice DC flow is almost automatically present and can be increased by a geometrical asymmetry.

In practice, heat is exchanged between the gas and the tube's wall and the regenerator. In the regenerator for instance, (without a DC flow) the heat absorbed by the regenerator during the compression phase and the heat absorbed by the gas flow during the expansion phase lead to one temperature profile along the regenerator. With an additional DC flow the tube and regenerator wall temperatures are affected. More gas passes the regenerator in one direction than in the other, modifying the temperature gradient along the regenerator. Duband et al. [16] have measured the wall temperature profiles of the regenerator and tube with an asymmetric bypass orifice. The temperature of the regenerator was cold along two third of its length, while the temperature of the tube was warm along two third of its length. Turning the bypass orifice resulted in the opposite, a DC flow through the bypass via the tube, regenerator again to the bypass.

## Chapter 6

# Conclusions

Three types of miniature pulse tube coolers have been investigated: the orifice, the inertance and the double inlet pulse tube cooler. From this study the following conclusions can be drawn:

- Miniature pulse tube coolers refrigerate. Temperatures below 80 K have been reached and with some modifications considerable cooling power at 80 K must be possible.
- Three orifice diameters have been tested. The experiments showed that the best performing orifice in an orifice pulse tube cooler has a phase angle  $\theta_L$  between  $40^\circ$  and  $45^\circ$ .
- A higher frequency increases the optimal orifice diameter. A tube volume of  $1.6 \text{ cm}^3$  or  $2.0 \text{ cm}^3$  has a best performing orifice diameter of 0.35 mm if the frequency is 35 Hz or 40 Hz. The same or better results can be obtained with an orifice diameter of 0.4 mm if the frequency is 45 Hz.
- Cooling power is mainly obtained by means of an adiabatic enthalpy flow through the core of the tube. The enthalpy flow consists of three components: the adiabatic enthalpy flow, surface heat pumping and the gradient effect. Surface heat pumping and the gradient effect are obtained in the thermal boundary layer  $\delta_T$  (typically 5 to 10 % of the tube's radius) near the wall. The gradient effect is generally more negative than surface heat pumping is positive.
- The cooling power increases linear with the cold heat exchanger temperature  $T_L$ . If  $T_L$  increases the pressure amplitude in the tube and the amplitude of the volume flow through the tube increase, resulting in an increasing enthalpy flow through the tube. If  $T_L$  increases the temperature difference over both the tube's wall and the regenerator decrease, decreasing the losses as the heat conduction decreases and the enthalpy flow through the regenerator decreases.
- In the measured range of 1.2 MPa to 2.8 MPa, a higher mean pressure results in an increasing cooling power per kelvin, if the mechanical input power is constant. The coefficient of performance  $\xi$  increases with an increasing mean pressure.
- In the measured range of 10 W to 35 W, a higher mechanical input power results in an increasing cooling power per kelvin and a decreasing minimum cold heat exchanger temperature, if the mean pressure is constant. The  $\Delta\langle\dot{Q}\rangle/\Delta T_L$  per mechanical input watt decreases if the mechanical input power increases.



- Lower temperatures have been reached with an inertance pulse tube cooler than with an orifice pulse tube cooler. With the optimal performance conditions, the phase angle has been found to be around  $30^\circ$  in the inertance pulse tube cooler.
- There is an inertance length interval where approximately the same cold heat exchanger temperatures can be reached. This length interval increases when the inertance diameter is increased.
- A higher mean pressure increases the optimum length of the inertance. A larger inertance diameter also results in a larger optimum length of the inertance. A higher frequency results in a smaller optimum length of the inertance.
- It has been found that an inertance diameter of 0.91 mm and a length around 1.5 m, or an inertance diameter of 0.79 mm and a length around 0.5 m reach the lowest temperatures if the tube's volume is  $1.6 \text{ cm}^3$ . This has been found for a frequency of 35 Hz and a mean pressure of 1.2 MPa, 1.6 MPa and 2.0 MPa. It has also been found that an inertance diameter of 1.32 mm is too large for a tube volume of  $1.6 \text{ cm}^3$ . If the tube volume is  $2.0 \text{ cm}^3$ , an inertance diameter of 1.02 mm and a length around 1.7 m has been found to reach the lowest temperatures. This has been found for a frequency of 35 Hz and a mean pressure of 2.4 MPa and 2.8 MPa.
- The use of a bypass orifice is beneficial in both an orifice and an inertance pulse tube cooler as lower cold heat exchanger temperatures can be reached. With a bypass orifice the pressure amplitude in the tube increases with approximately 5 %.
- It has been found that the best performing bypass orifice diameter is independent of the mean pressure, in the measured range of 1.2 MPa to 2.0 MPa.
- It has been found that the best performing bypass orifice diameter is the same for an orifice and an inertance pulse tube cooler. In both cases the best performing orifice or the best performing inertance has been used.
- The use of a bypass orifice can introduce a DC flow.
- A filling factor  $f=0.22$  is too small. A filling factor  $f=0.29$  gives better results.

The obtained results result in the following recommendations:

- A heat exchanger at the warm end of the regenerator will increase the performance of the cooler. The warm end temperature of the regenerator will drop, decreasing the heat conduction to the cold heat exchanger and decreasing the enthalpy flow through the regenerator.
- Use a capillary as the bypass instead of a bypass orifice. It is easier to make a symmetric capillary than it is to make a symmetric orifice. When a small diameter is used, the flow resistance can be varied, by varying the length and there is almost no inductance.
- Use a 55 mm pulse tube length instead of a tube length of 70 mm. With a smaller tube volume the pressure amplitude will be larger when the same mechanical input power is applied. As a regenerator length is used of 55 mm combined with a filling factor around 0.29, the empty space will be smaller than in the tested 70 mm regenerator. The accumulation of gas in the regenerator will decrease, resulting in a higher volume flow at the cold side of the pulse tube. If the experiments would show that the enthalpy flow through the regenerator is large the filling factor could be increased but the regenerator could also be made longer.
- A heat exchanger at the warm end of the tube will increase the performance of the cooler. This is of more use when an inertance is used than when an orifice is used. If the gas leaving the tube at the warm side does not mix with the gas in the buffer the warm end temperature of the tube increases. With the aid of a heat exchanger the heat can be rejected to the surroundings, decreasing the warm end temperature. The enthalpy flow through the tube increases and the heat conduction through the tube's wall decreases.



## References

- [1] R. Radebaugh, Recent developments in cryocoolers, 19<sup>th</sup> Int. Congress of Refrigeration **3b** (1995), 973.
- [2] W.E. Gifford, R.C. Longworth, Pulse-tube refrigeration, Advances in cryogenic engineering **10B** (1963), 69.
- [3] E.I. Mikulin, A.A. Tarasov, M.P. Shkrebyonock, Low temperature expansion pulse tubes, Advances in cryogenic engineering **29** (1984), 629.
- [4] S. Zhu, P. Wu, Z. Chen, Double inlet pulse tube refrigerators: an important improvement, Cryogenics **30** (1990), 514.
- [5] K.Kanao, N. Watanabe, Y. Kanazawa, A miniature pulse tube refrigerator for temperatures below 100 K, Cryogenics **34** (1994), 167.
- [6] P.P. Steijaert, Thermodynamical aspects of pulse-tube refrigerators, Technische Universiteit Eindhoven (1999).
- [7] A.T.A.M. de Waele, P.P. Steijaert, J.J. Koning, Thermodynamical aspects of pulse tubes II, Cryogenics **38** (1998), 329.
- [8] G.W. Swift, Thermoacoustic engines, Journal of Acoustic Society of America **84** (1988), 1145.
- [9] P.R. Roach, A. Kashani, Pulse tube coolers with an inertance tube: theory, modeling, and practice, Advances in cryogenic engineering **43** (1998), 1895.
- [10] R. Radebaugh, Comparison of models for inertance tubes, Presented at the 10<sup>th</sup> International Cryocooler Conference (1998), to be published.
- [11] A.T.A.M. de Waele, H.W.G. Hooijkaas, P.P. Steijaert, A.A.J. Benschop, Regenerator dynamics in the harmonic approximation, Cryogenics **38** (1998), 995.
- [12] J. Gijzen, Analytical and experimental investigation of a miniature pulse-tube refrigerator, Technische Universiteit Eindhoven (1995).
- [13] M.L. Bosgra, Dynamic analysis of a rod driven displacer in a Stirling cryocooler, Universiteit Twente (1996).
- [14] I.E. Idelchik, Handbook of hydraulic resistance: second edition, revised and augmented, Hemisphere publishing corporation (1986), Chapter 4.
- [15] H.W.G. Hooijkaas, A.A.J. Benschop, Pulse tube development using harmonic simulations, Presented at the 10<sup>th</sup> International Cryocooler Conference (1998), to be published.
- [16] L. Duband, I. Charles, A. Ravex, L. Miquet, C. Jewell, Experimental results on inertance and permanent flow in pulse tube coolers, Presented at the 10<sup>th</sup> International Cryocooler Conference (1998), to be published.